

U.S. DEPARTMENT OF COMMERCE  
National Technical Information Service

AD-A027 958

CHARACTERISTIC STEADY-STATE ELECTRON EMISSION  
PROPERTIES FOR PARAMETRIC BLACKBODY X-RAY  
SPECTRA ON SEVERAL MATERIALS

MISSION RESEARCH CORPORATION

PREPARED FOR  
DEFENSE NUCLEAR AGENCY

FEBRUARY 1976

## **REPRODUCTION QUALITY NOTICE**

This document is the best quality available. The copy furnished to DTIC contained pages that may have the following quality problems:

- Pages smaller or larger than normal.
- Pages with background color or light colored printing.
- Pages with small type or poor printing; and or
- Pages with continuous tone material or color photographs.

Due to various output media available these conditions may or may not cause poor legibility in the microfiche or hardcopy output you receive.



If this block is checked, the copy furnished to DTIC contained pages with color printing, that when reproduced in Black and White, may change detail of the original copy.

224208

DNA 3931T

**CHARACTERISTIC STEADY-STATE  
ELECTRON EMISSION PROPERTIES FOR  
PARAMETRIC BLACKBODY X-RAY  
SPECTRA ON SEVERAL MATERIALS**

X  
M  
C  
S  
C  
O  
A  
D  
A  
1  
0  
2  
7  
9  
1

Mission Research Corporation  
735 State Street  
Santa Barbara, California 93101

February 1976

Topical Report

CONTRACT No. DNA 001-76-C-0086

APPROVED FOR PUBLIC RELEASE;  
DISTRIBUTION UNLIMITED.

THIS WORK SPONSORED BY THE DEFENSE NUCLEAR AGENCY  
UNDER R&D&E RMSS CODE B327076464 R99QAXEB06964 H25900.

Prepared for  
Director  
**DEFENSE NUCLEAR AGENCY**  
Washington, D. C. 20305

REPRODUCED BY  
**NATIONAL TECHNICAL  
INFORMATION SERVICE**  
U. S. DEPARTMENT OF COMMERCE  
SPRINGFIELD, VA 22161

UNCLASSIFIED

SECURITY CLASSIFICATION OF THIS PAGE (When Data Entered)

DD FORM 1 JAN 71 1473 EDITION OF 1 NOV 65 IS OBSOLETE

UNCLASSIFIED

SECURITY CLASSIFICATION OF THIS PAGE (When Data Entered)

## TABLE OF CONTENTS

	PAGE
ILLUSTRATIONS	2
SECTION 1—INTRODUCTION	5
THEORETICAL ASSUMPTIONS	6
SECTION 2—ELECTRON YIELDS AND ENERGY SPECTRA	9
SECTION 3—TIMES OF VALIDITY OF STEADY-STATE THEORY	20
A. Transient Build-Up to Steady State	21
B. Maintenance of Quasi-Steady State	26
SECTION 4—DEBYE LENGTHS	31
SECTION 5—ELECTRON NUMBER DENSITY AT SURFACE	36
SECTION 6—ELECTRON NUMBER DENSITY PROFILE	40
INTEGRATED NUMBER DENSITY	43
SECTION 7—ELECTRIC FIELD AT SURFACE	45
SECTION 8—ELECTRIC FIELD PROFILE	49
SECTION 9—PLASMA FREQUENCY AT SURFACE	51.
SECTION 10—DIPOLE MOMENT PER UNIT AREA	55
SECTION 11—EXAMPLE	58
REFERENCES	62

## LIST OF ILLUSTRATIONS

FIGURE		PAGE
1	Total backscattered electron yield for incident blackbody spectrum.	11
2	Electron spectra, 1 keV incident blackbody.	12
3	Electron spectra, 2 keV incident blackbody.	13
4	Electron spectra, 3 keV incident blackbody.	14
5	Electron spectra, 5 keV incident blackbody.	15
6	Electron spectra, 8 keV incident blackbody.	16
7	Electron spectra, 10 keV incident blackbody.	17
8	a. $t_s$ for Aluminum.	23
8	b. $t_s$ for Gold.	24
8	c. $t_s$ for Silicon Dioxide.	25
9	a. $t_{ret}$ for Aluminum.	28
9	b. $t_{ret}$ for Gold.	29
9	c. $t_{ret}$ for Silicon Dioxide.	30
10	a. Debye lengths for Aluminum.	33
10	b. Debye lengths for Gold.	34
10	c. Debye lengths for Silicon Dioxide.	35
11	a. Surface electron density for Aluminum.	37
11	b. Surface electron density for Gold.	38

FIGURE	PAGE
11      c. Surface electron density for Silicon Dioxide.	39
12      Normalized electron density profile.	41
13      Normalized electron density profile.	42
14      Fraction of electrons out to x.	44
15      a. Surface electric field for Aluminum.	46
15      b. Surface electric field for Gold.	47
15      c. Surface electric field for Silicon Dioxide.	48
16      Normalized electric field profile.	50
17      a. Surface plasma frequency for Aluminum.	52
17      b. Surface plasma frequency for Gold.	53
17      c. Surface plasma frequency for Silicon Dioxide.	54
18      Normalized dipole moment per unit area.	56
19      X-ray time history for illustrative example.	59

## SECTION 1

### INTRODUCTION

To estimate the properties of the electron boundary layer produced when X rays fall on a material surface, it is helpful to have available tables and curves of useful boundary layer properties when a parametric set of photon spectra is incident on common materials.

This note collects some boundary layer properties for backscattered electrons for the cases in which blackbody photon sources of temperatures  $KT = 1, 2, 3, 5, 8$ , and  $10 \text{ keV}$  are normally incident on aluminum, gold, and silicon dioxide. For reasons discussed below the curves presented are for the case of a steady-state boundary layer, that is, it is assumed that conditions are not changing with time.

The electron properties given are:

1. Photoelectric yield, and backscattered electron energy spectra (Section 2);
2. Conditions for which steady state theory is valid (Section 3);
3. Boundary layer Debye lengths (Section 4);
4. Electron number density at the surface (Section 5);
5. Electron number density profile and the integrated density (Section 6);
6. Electric field at the surface (Section 7);

**Preceding page blank**

7. Electric field profile (Section 8);
8. Plasma frequency at the surface (Section 9);
9. Electric dipole moment per unit area (Section 10).

In Section 11 we give an example that illustrates the use of the graphs.

The graphs given here are meant to provide the reader with a ready reference for estimating boundary layer properties for incident photon spectra approximating blackbodies when steady-state conditions are valid.

### THEORETICAL ASSUMPTIONS

The exact conditions prevailing when an X-ray beam is incident on a material surface can vary widely. The incident photon pulse can have any time history and any energy spectrum, and the energy spectrum can itself vary with time. The angle of incidence and the physical size and shape of the target can also vary widely.

It would clearly be a difficult and lengthy task to parametrize all of these variables, tantamount to solving the general problem. Here we choose a more modest goal. We restrict attention to normal angles of incidence, and targets that are flat surfaces with dimensions large compared to the thickness of the boundary layer. This last assumption permits a one-dimensional theoretical treatment.

In addition, we choose for the energy spectrum a blackbody spectrum independent of time. This is partly because of its universal availability (theoretically) and similarity to some experimental sources of interest, and partly because a blackbody photon spectrum produces a backscattered electron energy spectrum which is very nearly exponential (see Section 2),

and the steady-state boundary layer structure for an exponential electron spectrum is known<sup>1</sup>.

A parametric study using monoenergetic X rays would not be particularly useful unless one were actually interested in the response to monoenergetic X rays. Since the boundary layer problem is a non-linear one, it is not possible to determine the response to a spectrum by superposing the responses to monoenergetic photons.

Even with these restrictions, the photon source can have an arbitrary time history. The solution for the time-dependent boundary layer structure even in one dimension is very difficult, and until a thorough study of this problem is made we find it wise to restrict parametric studies to the time-independent, or steady-state, case. Many photon sources of interest, while varying with time, vary slowly enough so that steady-state theory is approximately applicable at every instant of time using the instantaneous value of the X-ray flux.

Hence, in spite of the above stated restrictions, the graphs presented in this report should be useful for estimating boundary layer properties in many experimental situations of interest.

We have mentioned that a blackbody photon spectrum produces a backscattered electron energy spectrum that is very nearly exponential. It also turns out that the electron angular distribution is very nearly a  $\cos\theta$  distribution. The steady-state boundary layer theory for this case of exponential energy spectrum and  $\cos\theta$  angular distribution was presented in Reference 1. The graphs in the present report were constructed from the formulae given there.

In Figures 8, 9, 10, 11, 15, and 17, information has been compressed by using the top and right scales as well as the bottom and left scales. The top scale should be used with the right scale, and the bottom scale should be used with the left scale.

## SECTION 2

### ELECTRON YIELDS AND ENERGY SPECTRA

The backscattered electron yields and energy spectra depend only on the X-ray energy spectrum and angle of incidence and on the surface material. (For a thin surface they also depend on the material thickness. Here we assume the material is at least one electron range thick, and they are therefore independent of thickness.) They do not depend on the X-ray time history, and hence can be discussed independently of any dynamical assumptions about the boundary layer.

The photoelectric yields and backscattered electron energy spectra were computed using the electron transport code QUICKE2<sup>2</sup>. The photoelectric yields (or "efficiencies") are listed in Table 1 in units of electrons per photon and in units of electrons per calorie of incident fluence. These same backscattered yields are shown as a continuous function of incident blackbody temperature in Figure 1 (in units of electrons per calorie only).

The backscattered electron energy distributions are shown in Figures 2 through 7 for the six blackbody temperatures chosen. The ordinates are in units of electrons/keV per calorie incident fluence. Figures 2 through 7 are partially smoothed from the output of QUICKE2.

It is seen from these figures that, except for certain jumps at low energies caused by Auger electrons (at 1.4 keV in Aluminum and 8.25 keV in Gold), the electron energy spectra are nearly exponential with some characteristic energy  $E_1$ ,

Table 1. Backscattered electron efficiencies.

Incident Photon Blackbody Temperature (keV)	Aluminum		Gold		Silicon Dioxide	
	elecs/phot	elecs/cal.	elecs/phot	elecs/cal.	elecs/phot	elecs/cal.
1	3.55(-3)	3.04(13)	1.36(-2)	1.16(14)	2.69(-3)	2.30(13)
2	2.70(-3)	1.25(13)	1.55(-2)	7.21(13)	1.91(-3)	8.86(12)
3	2.06(-3)	6.49(12)	1.48(-2)	4.66(13)	1.42(-3)	4.49(12)
5	1.34(-3)	2.57(12)	1.30(-2)	2.50(13)	9.08(-4)	1.74(12)
8	8.56(-4)	1.03(12)	1.11(-2)	1.33(13)	5.76(-4)	6.94(11)
10	6.73(-4)	6.49(11)	1.01(-2)	9.71(12)	4.51(-4)	4.35(11)

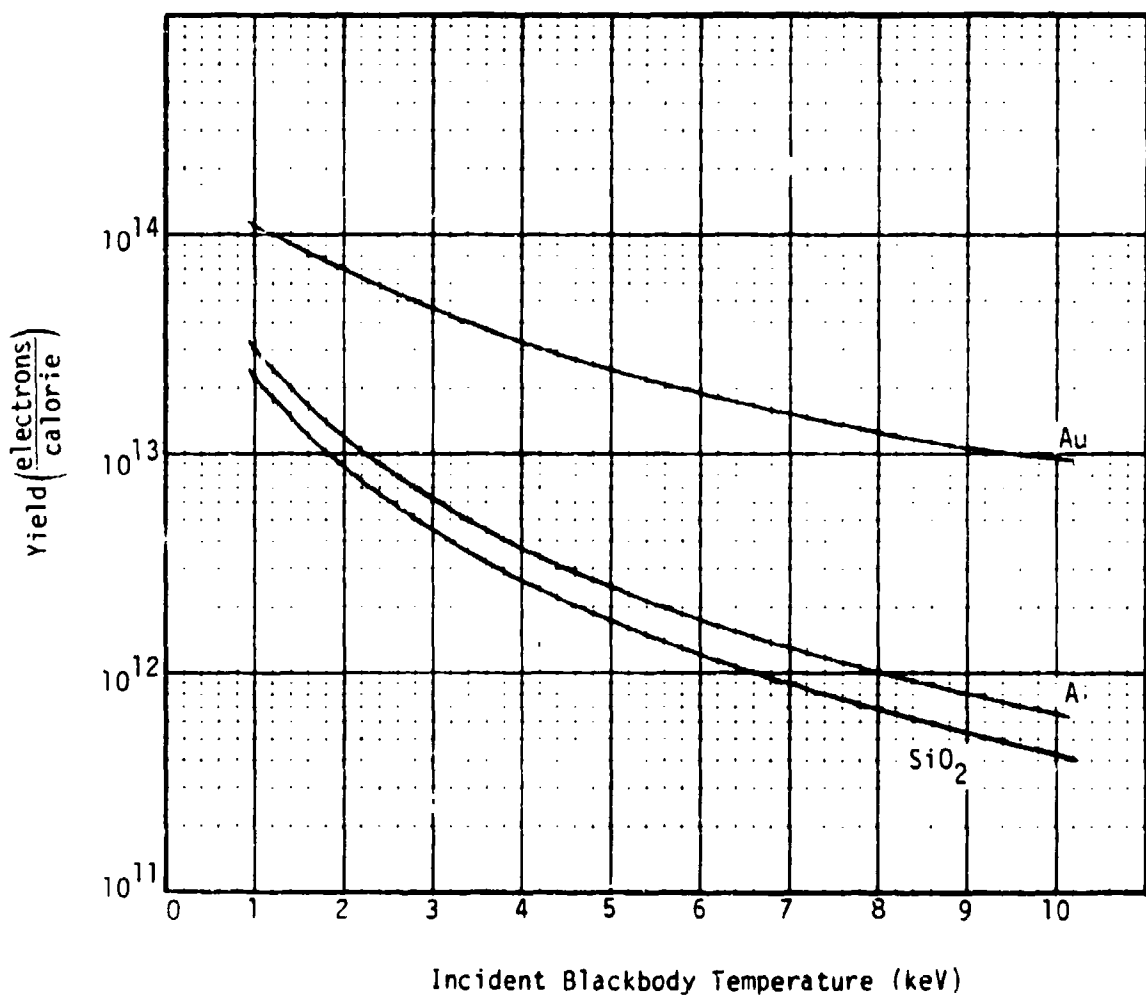


Figure 1. Total backscattered electron yield for incident blackbody spectrum.

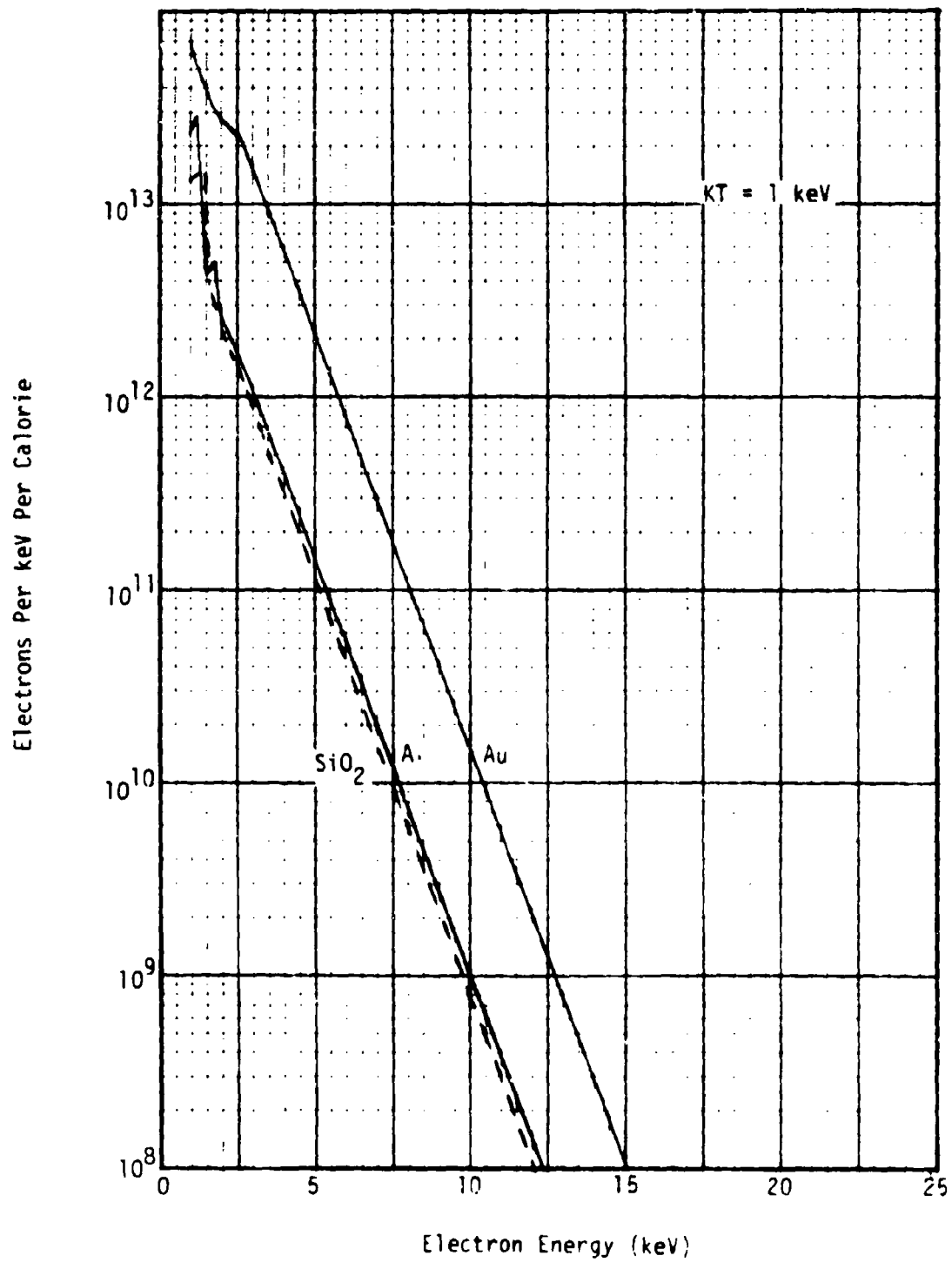


Figure 2. Electron spectra, 1 keV incident blackbody.

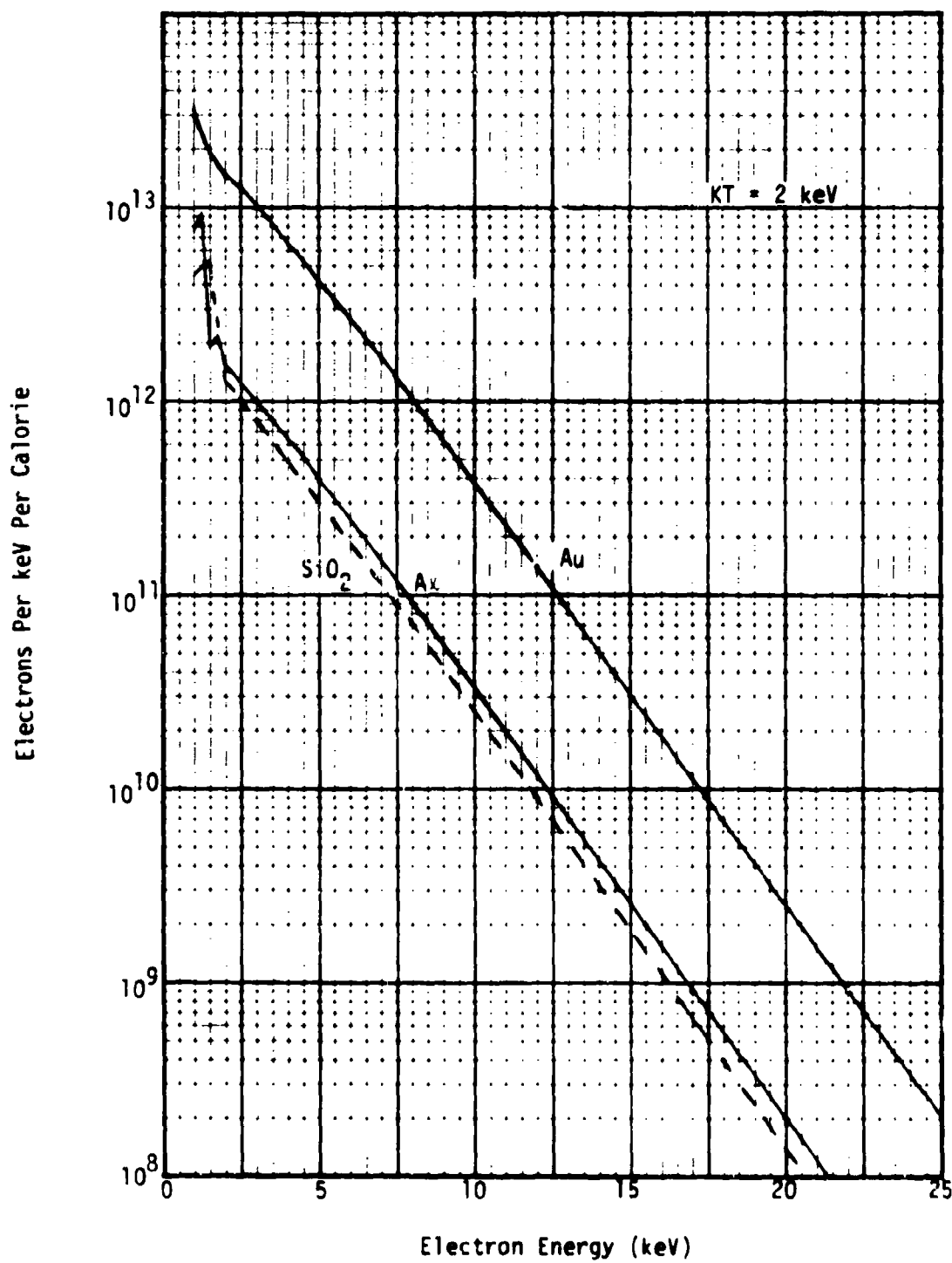


Figure 3. Electron spectra, 2 keV incident blackbody.

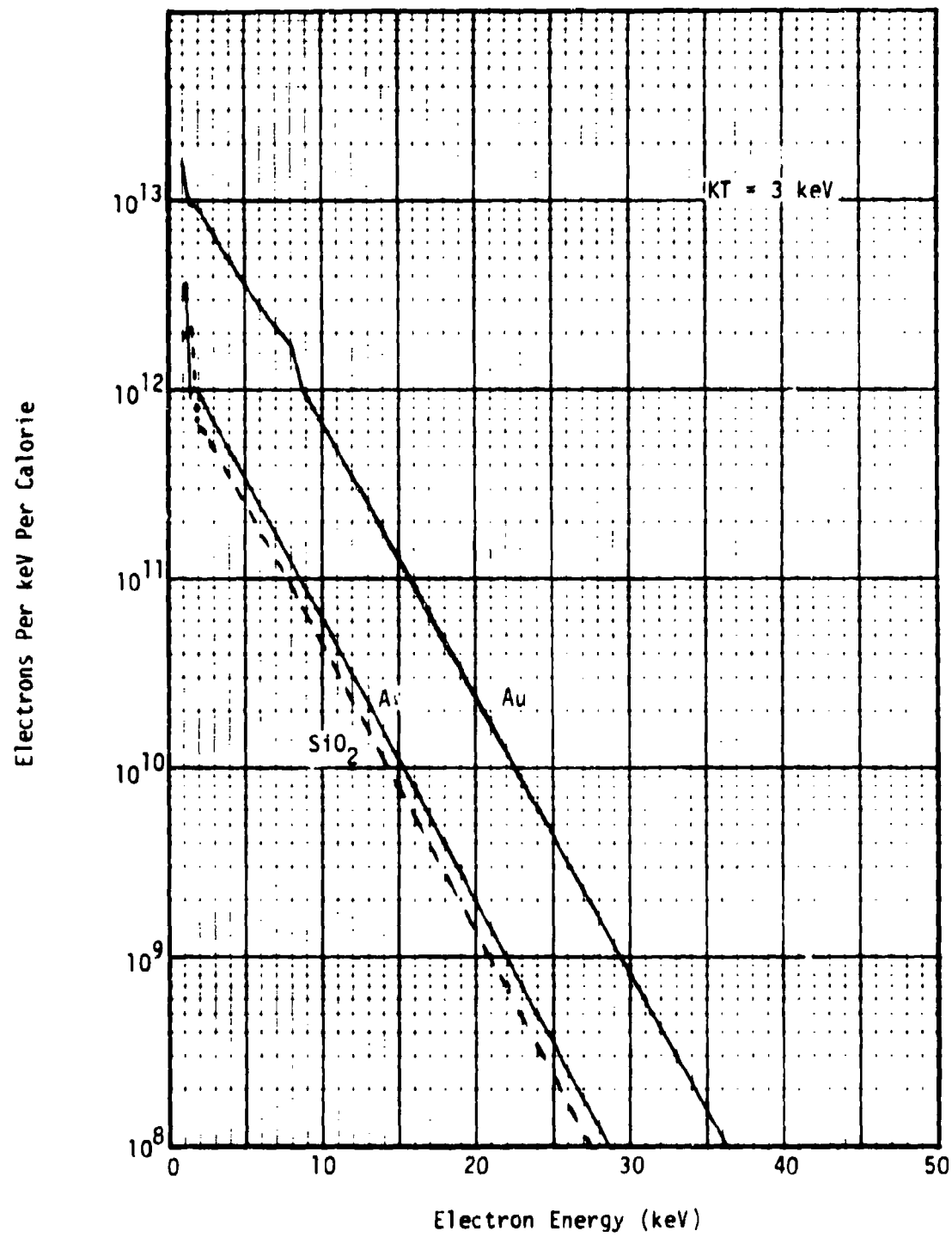


Figure 4. Electron spectra, 3 keV incident blackbody.

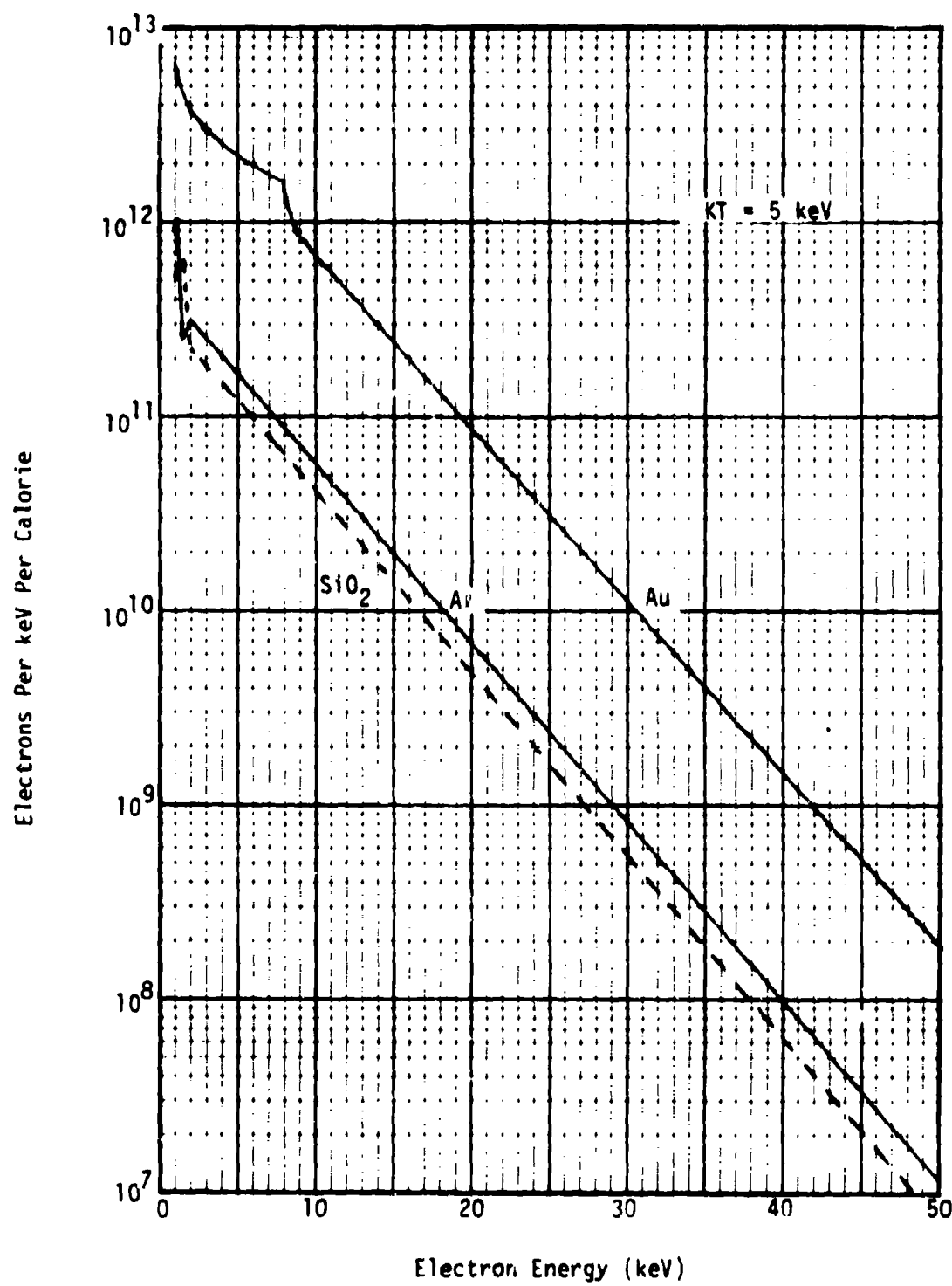


Figure 5. Electron spectra, 5 keV incident blackbody.

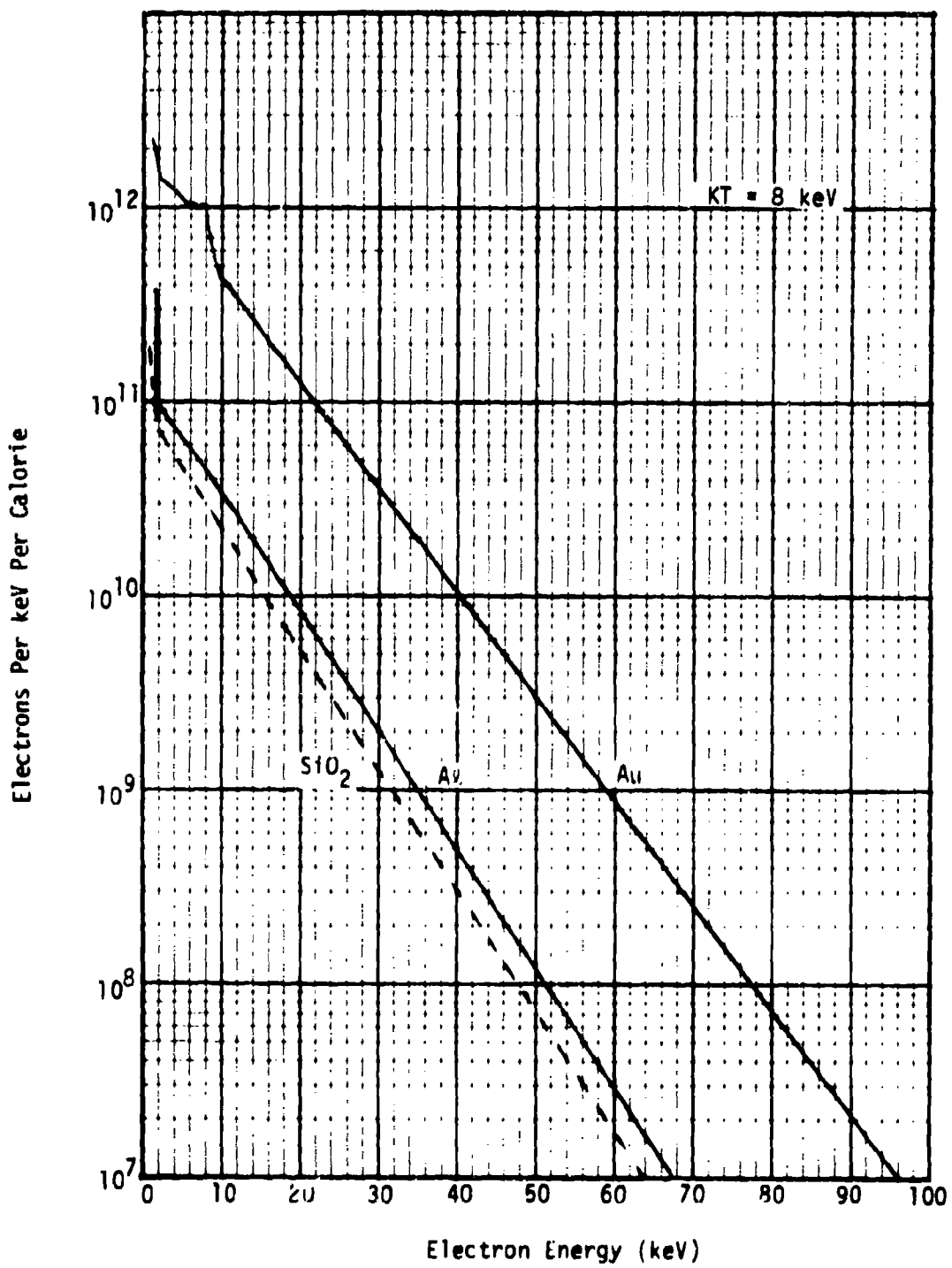


Figure 6. Electron spectra, 8 keV incident blackbody.

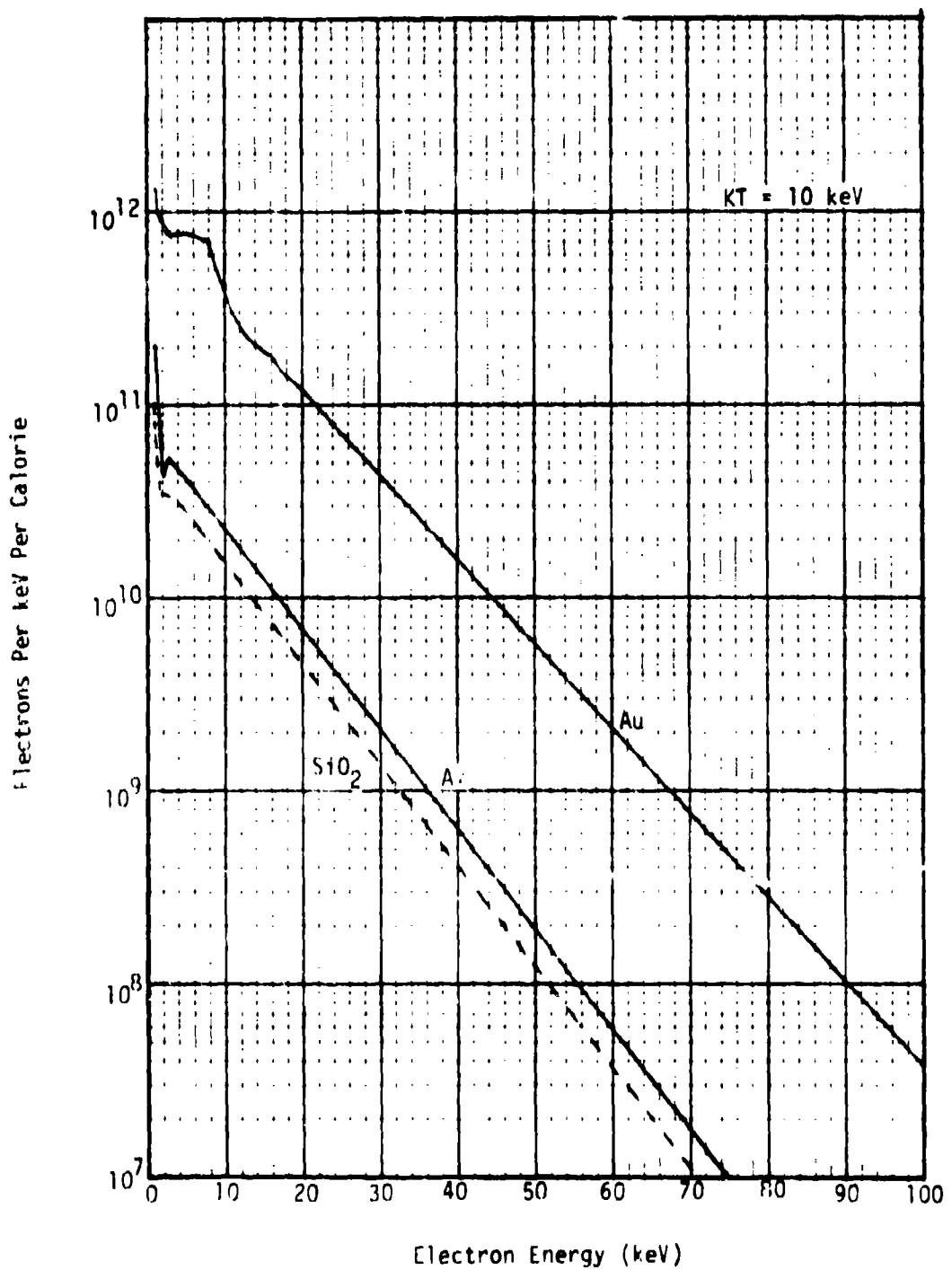


Figure 7. Electron spectra, 10 keV incident blackbody.

$$\frac{dn}{dE} \sim e^{-E/E_1} \text{ electrons/keV/unit fluence ,}$$

where E is the electron energy. By fitting a straight line to Figures 2 through 7, ignoring the Auger edges, we have determined values for  $E_1$ . These are listed in Table 2. The energies  $E_1$  are not very different from the temperature  $KT$ , and are nearly independent of target material. Using electron energy spectral response to monoenergetic photons, and superposing a blackbody spectrum, it is not hard to show that the electron spectrum should indeed be nearly exponential with exponentiation energy approximately equal to  $KT$ , as has been discussed by Higgins<sup>3</sup>.

Table 2. Exponentiation energies,  $E_1$ , for backscattered electrons.

Incident Photon Blackbody Temperature (keV)	Exponentiation Energy, $E_1$ (keV)		
	Aluminum	Gold	Silicon Dioxide
1	1.02	1.01	0.98
2	2.09	2.05	1.97
3	2.96	2.99	2.86
5	4.77	4.87	4.63
8	7.27	7.95	6.79
10	8.69	10.07	8.36

### SECTION 3

#### TIMES OF VALIDITY OF STEADY-STATE THEORY

For a given X-ray pulse there are two characteristic times that determine whether or not steady-state theory is applicable.

The first electrons ejected by the arriving X-ray pulse are certainly not in steady state. Some time,  $t_s$ , must pass after the X rays first arrive before the boundary layer will have achieved a steady or quasi-steady state. There will be a transient build-up to steady state. We may expect this time  $t_s$  to depend on the fluence and the rise time of the incident pulse.

Once this transient build-up is over, we will achieve a steady state and stay in a (quasi-) steady state only if the X-ray pulse is not changing too rapidly in time. Each ejected electron takes a certain time,  $t_{ret}$ , to reach its maximum distance from the surface, turn around, and return to the surface. Steady-state formulae will be applicable after time  $t_s$  only if the incident pulse changes only slightly during the time  $t_{ret}$  that it takes an electron of, say, average energy to return. Thus the boundary layer will maintain a (quasi-) steady-state structure with the instantaneous value of the flux only if the flux is nearly constant over the time  $t_{ret}$ .

Hence, for a given pulse time history, one must estimate both  $t_s$  and  $t_{ret}$ . We now discuss these two times more quantitatively.

### A. Transient Build-Up to Steady State

Let  $\phi(t)$  be the X-ray fluence [ $\text{cal}/\text{cm}^2$ ] that has arrived up to time  $t$ . Then the X-ray flux is

$$\dot{\phi} = \frac{d\phi}{dt} [\text{cal}/\text{cm}^2/\text{sec}] . \quad (1)$$

Let  $Y$  [electrons/cal] be the photoelectric yield as given in Table 1 or Figure 1. Then electrons are emitted at a rate

$$r_0 = Y\dot{\phi} [\text{electrons}/\text{cm}^2/\text{sec}] , \quad (2)$$

and

$$N(t) = \int_0^t r_0 dt [\text{electrons}/\text{cm}^2] , \quad (3)$$

are emitted by time  $t$ .

Now Reference 1 shows that, for an exponential electron energy spectrum with exponentiation energy  $E_1$  and a  $\cos\theta$  angular distribution, the number of electrons required for steady state when the emission rate is  $r_0$  is

$$N_s = (r_0 \sqrt{2mE_1} / 3\sqrt{\pi} e^2)^{1/2} [\text{electrons}/\text{cm}^2] . \quad (4)$$

Steady state theory should begin to apply after the number of electrons ejected, Equation 3, exceeds that necessary for steady state, Equation 4. Hence, equating  $N(t)$  and  $N_s$  will determine the time  $t_s$ .

To simplify matters we assume the pulse is linearly rising,

$$\dot{\phi} = \ddot{\phi}t , \quad (5)$$

at a rate  $\ddot{\phi}$  [ $\text{cal}/\text{cm}^2/\text{sec}^2$ ], so that

$$N(t) = \frac{1}{2} Y \phi t^2 , \quad (6)$$

and

$$N_s = \left( \frac{\sqrt{2m} E_1 Y \phi t}{3\sqrt{\pi} e^2} \right)^{1/2} . \quad (7)$$

Equating these we obtain

$$\begin{aligned} t_s &= \left( \frac{4 \sqrt{2m} E_1}{3 \sqrt{\pi} e^2 \phi} \right)^{1/3} \\ &= 1.773 \times 10^{-6} \left( \frac{\sqrt{E_1 (\text{keV})}}{Y \left( \frac{\text{elec}}{\text{cal}} \right) \phi \left( \frac{\text{cal}}{\text{cm}^2 \text{ns}^2} \right)} \right)^{1/3} \text{ sec} . \end{aligned} \quad (8)$$

This is plotted as a function of  $\dot{\phi}$  [cal/cm<sup>2</sup>/nanosec<sup>2</sup>] in Figures 8a, b, and c for aluminum, gold, and silicon dioxide.

For example, if a 3 keV blackbody falls on gold and has a rise rate of  $10^{-6}$  cal/cm<sup>2</sup>/ns<sup>2</sup>, then Figure 8b shows  $t_s = 6$  ns.

Actually some of the electrons emitted by time  $t_s$ , Equations 3 or 6, will have returned so that the total number of electrons residing outside the surface at  $t_s$  will be less than  $N(t_s)$ . Hence it will take somewhat longer than  $t_s$  as given by Equation 8 before steady-state theory is fully applicable.

In addition, electrons emitted with energy less than  $E_1$  will be in steady state before  $t_s$  since their return time is less than that for electrons of energy  $E_1$ . Similarly, more energetic electrons than  $E_1$  will take longer to achieve steady state. Thus if one is interested in certain details of the boundary layer that depend on high energy electrons, such as the local electron number density far from the surface, one must wait

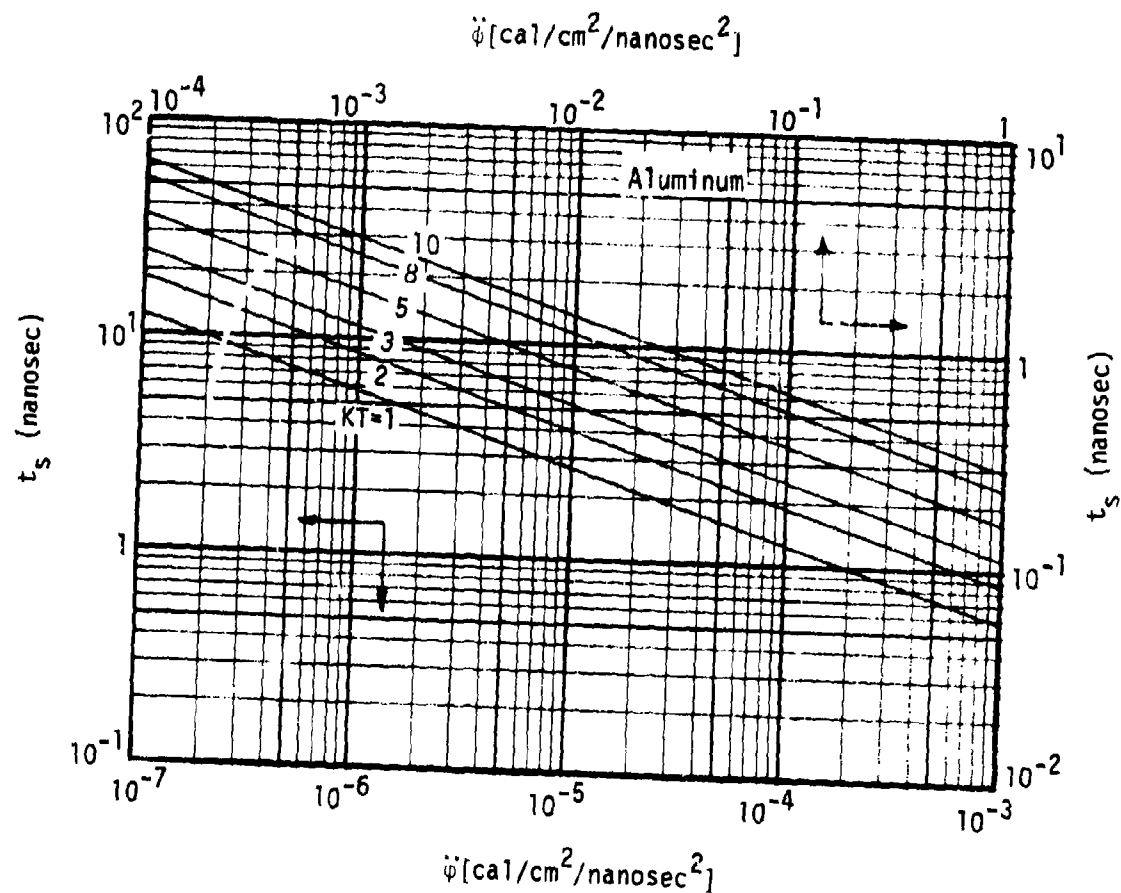


Figure 8a.  $t_s$  for Aluminum.

Numbers on curves are blackbody temperatures in keV.

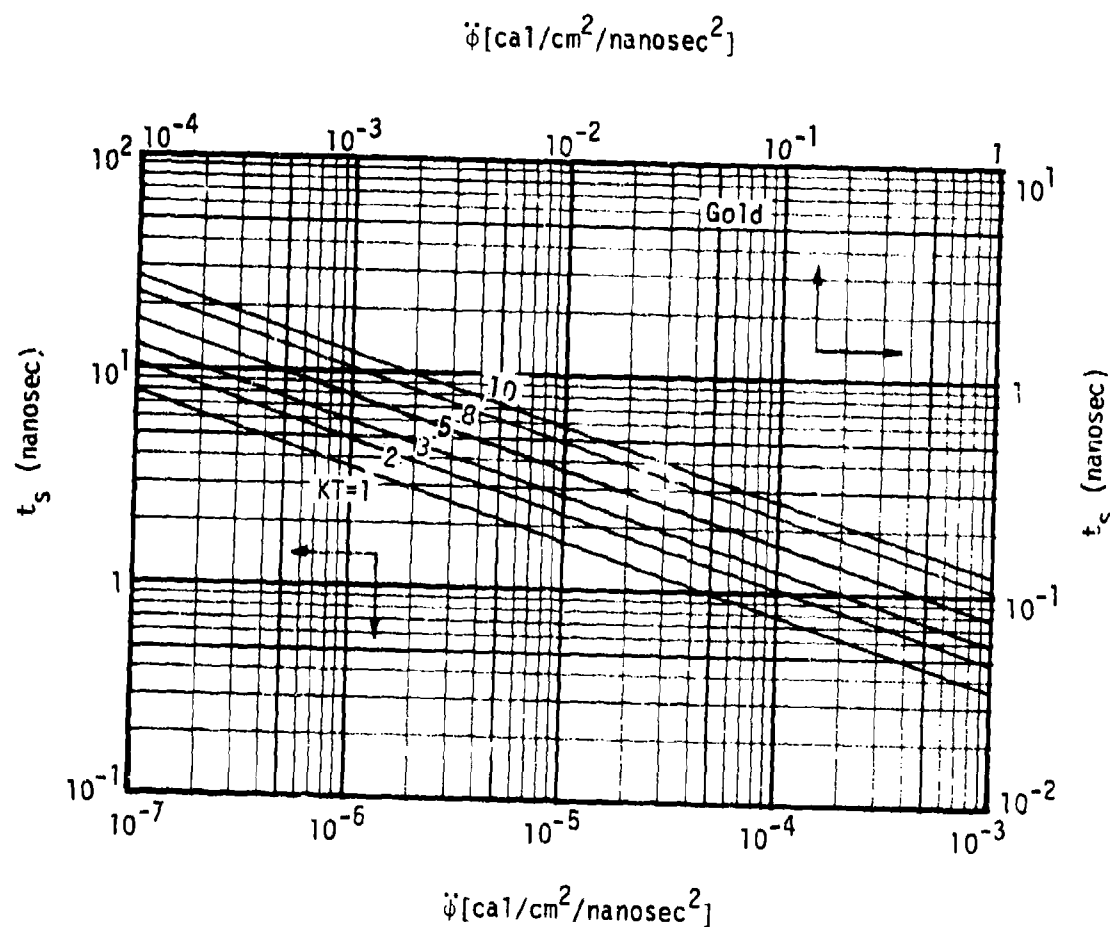


Figure 8b.  $t_s$  for Gold.

Numbers on curves are blackbody temperatures in keV.

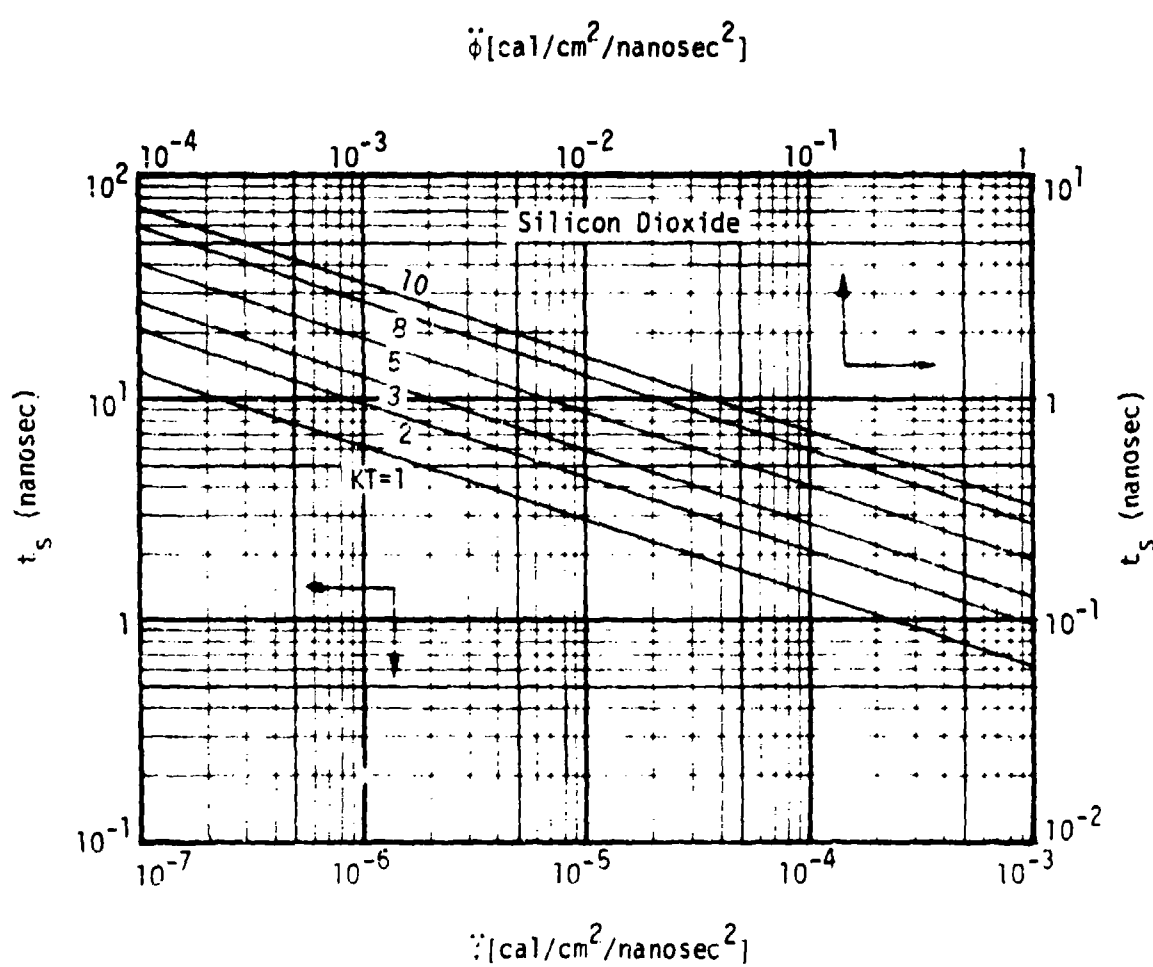


Figure 8c.  $t_s$  for Silicon Dioxide.

Numbers on curves are blackbody temperatures in keV.

longer than  $t_s$  before trusting steady-state expressions. Hence the precise value of  $t_s$  as given in Figures 8 must be used with care.

Fortunately many X-ray pulses last much longer than  $t_s$ , so that even with the above two caveats Figures 8 are useful.

In Figures 8a, b, and c, and all later figures marked with two pairs of arrows, the left-hand scale should be read with the lower scale, and the right-hand scale should be read with the upper scale.

### B. Maintenance of Quasi-Steady State

Steady-state theory with the instantaneous value of X-ray flux will remain applicable if the flux is nearly constant during the turn around time,  $t_{ret}$ , of an electron of average energy. From Reference 1, we find that an electron emitted with normal component of energy  $1/2 m v_x^2$ , where  $v_x$  is its normal velocity, equal to the average energy  $E_1$ ,

$$\frac{1}{2} m v_x^2 = E_1 , \quad (9)$$

will return in time

$$t_{ret} \approx S \frac{\zeta_D}{v_1} = \sqrt{2m v_1 / \pi^{3/2} e^2 r_0} , \quad (10)$$

where  $\zeta_D$  is the surface Debye length and  $v_1 = \sqrt{2E_1/m}$ . Using Equation 2, this can be written

$$t_{ret} = 5.158 \cdot 10^{-5} \left( \frac{\sqrt{E_1 (\text{keV})}}{\gamma \left( \frac{\text{elec}}{\text{cal}} \right) \left( \frac{\text{cal}}{\text{cm}^2 \text{ns}} \right)} \right)^{1/2} \text{ sec} , \quad (11)$$

BEST AVAILABLE COPY

This is shown as a function of the flux  $\dot{\phi} = d\phi/dt$  [cal/cm<sup>2</sup>/nanosec] in Figures 9a, b, and c.

For example if a 5 keV blackbody is illuminating aluminum at an instantaneous flux of  $10^{-2}$  cal/cm<sup>2</sup>/nanosec, Figure 9a shows that steady-state expressions should be valid if the flux does not change much over a time  $t_{ret} = 0.47$  nanosec.

Since electrons emitted with energy greater than  $E_j$  will have a longer return time, one must use a larger  $t_{ret}$  if one is interested in detailed steady-state quantities that depend on these higher energy electrons, such as the local electron number density far from the surface. If, however, one is interested in a quantity that is determined primarily by lower energy electrons, such as the local number density less than a Debye length from the surface, one may use a smaller  $t_{ret}$ .

For "global" or integrated quantities such as the surface electric field, (or, what is the same thing, the surface charge density or the total number of electrons outside the surface) the time  $t_{ret}$  plotted in Figures 9a, b, and c should be adequate.

From the given properties of the incident X-ray pulse one can determine  $t_s$  and  $t_{ret}$  from Figures 8 and 9. The graphs in the following sections will be valid for times greater than  $t_s$  if the flux is nearly constant over a time  $t_{ret}$ .

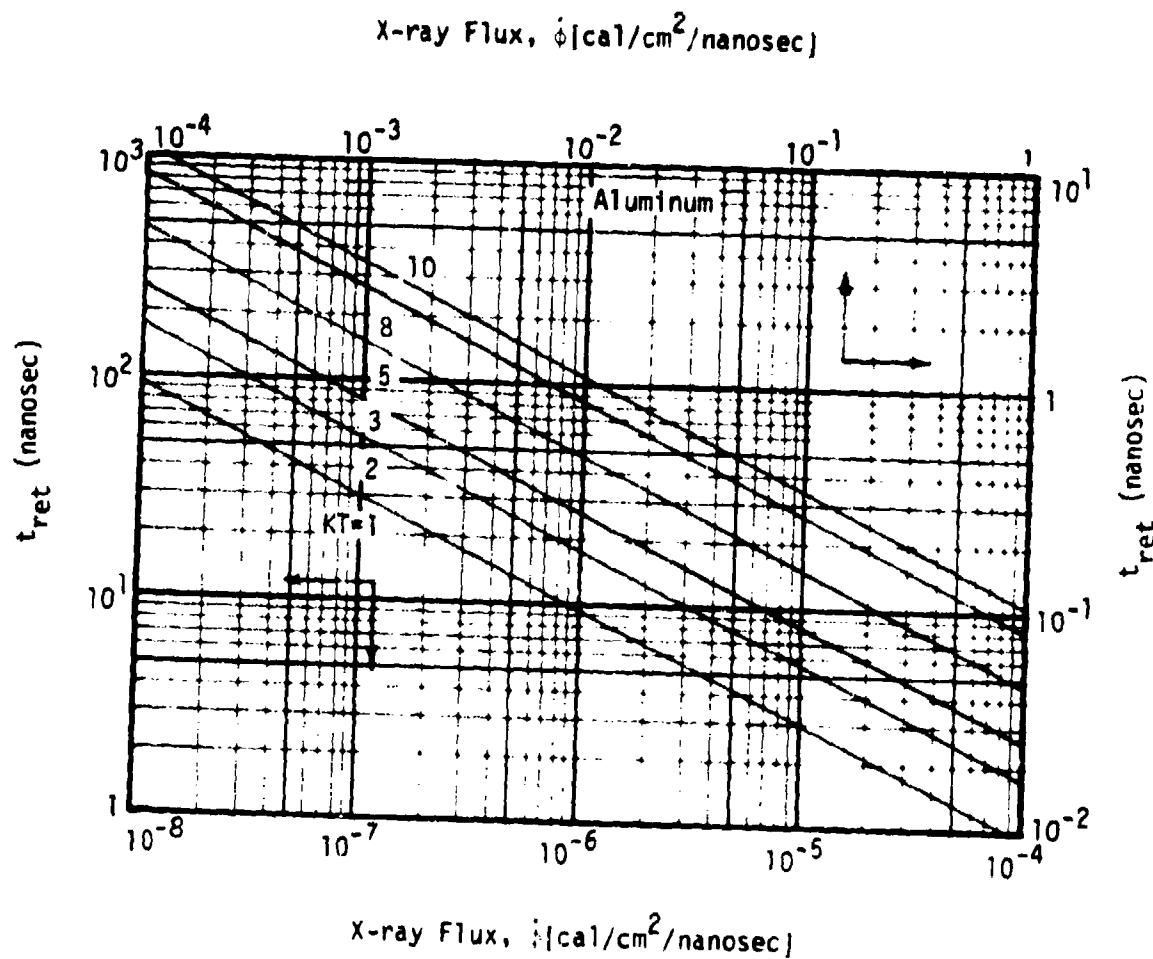


Figure 9a.  $t_{ret}$  for Aluminum.

Numbers on curves are blackbody temperatures in keV.

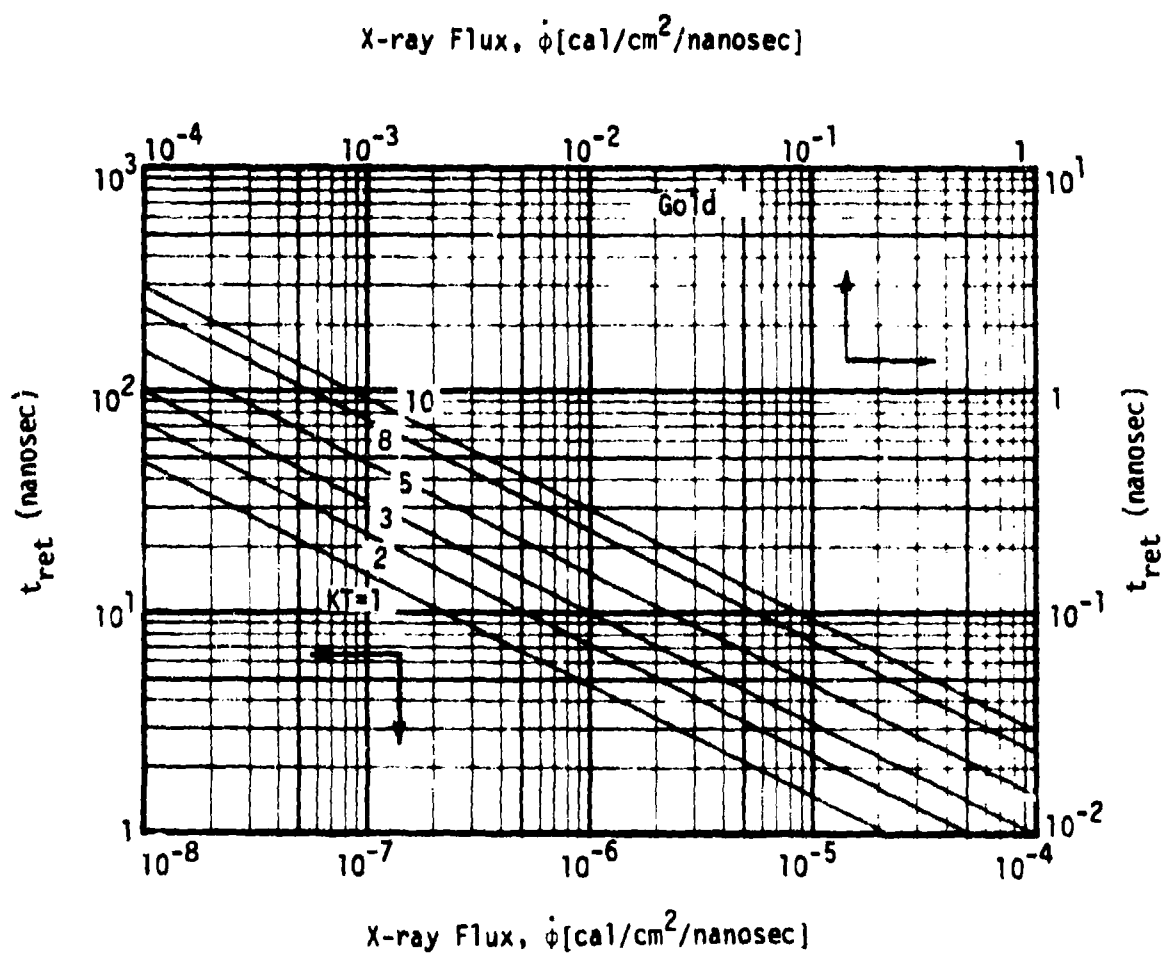


Figure 9b.  $t_{\text{ret}}$  for Gold.

Numbers on curves are blackbody temperatures in keV.

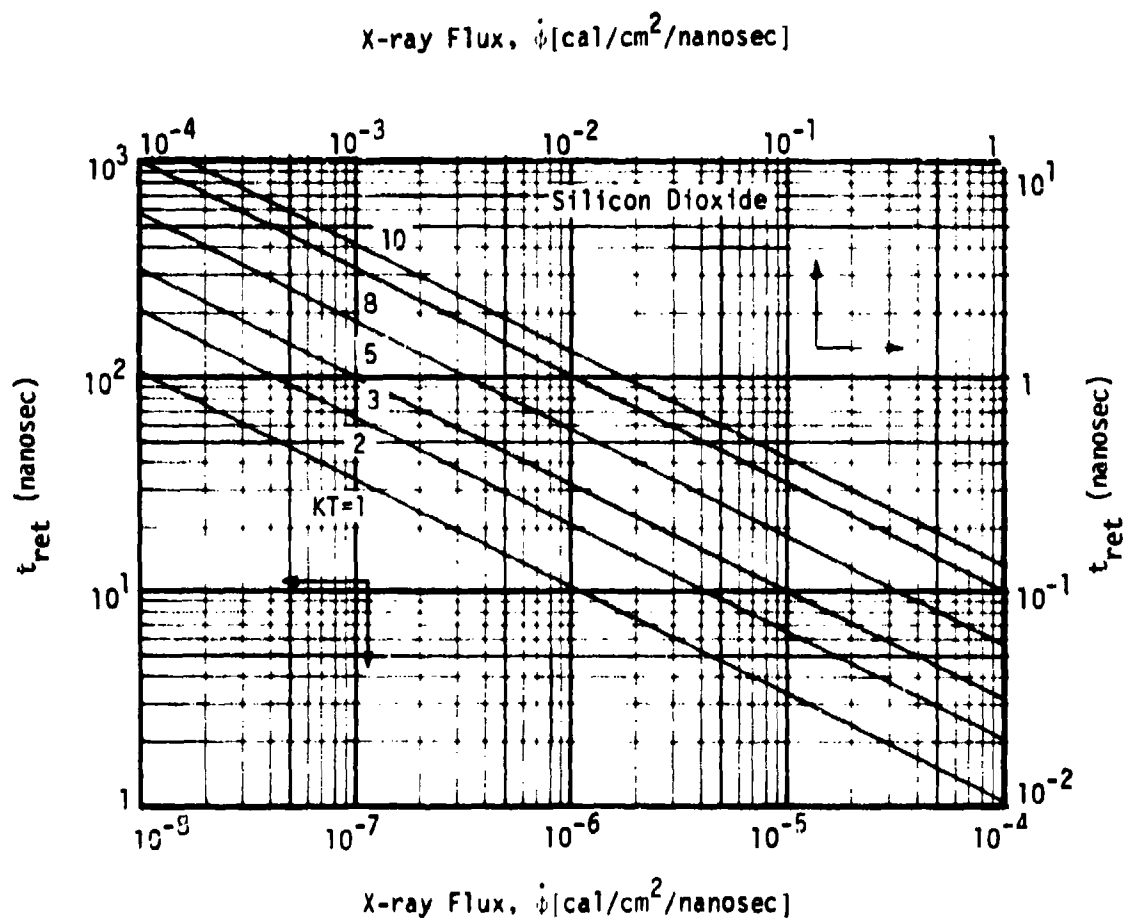


Figure 9c.  $t_{ret}$  for Silicon Dioxide.

Numbers on curves are blackbody temperatures in keV.

## SECTION 4

### DEBYE LENGTHS

The Debye length is the characteristic distance over which the properties of the boundary layer vary significantly. It is a measure of the "thickness" of the boundary layer. If  $w$  is a characteristic energy (ergs) of a plasma, and  $N$  is the electron number density ( $\text{cm}^{-3}$ ) then the Debye length is

$$\ell_D = \sqrt{\frac{w}{4\pi e^2 N}} \quad \text{cm} . \quad (12)$$

It is equal to a characteristic plasma velocity divided by the plasma frequency.

In the present context we use for  $w$  the exponentiation energy  $E_1$ . This is also the average electron energy. For  $N$  we take the value at the emission surface in steady state when the electron energy distribution is exponential and the angular emission distribution is  $\cos\theta^1$ . In this case

$$N = 4\sqrt{\pi} \frac{r_0}{v_1} , \quad (13)$$

where  $v_1 = \sqrt{2E_1/m}$  and  $r_0$  is given by Equation 2. Thus

$$\begin{aligned} \ell_D &= \left( \frac{E_1 \sqrt{2E_1/m}}{16\pi^{5/2} e^2 Y \phi} \right)^{1/2} \\ &= 1.209 \times 10^4 \left( \frac{E_1 (\text{keV})^{5/2}}{Y \left( \frac{\text{eV}}{\text{cal}} \right) \phi \left( \frac{\text{cal}}{\text{cm}^2 \text{ns}} \right)} \right)^{1/2} \text{cm} . \end{aligned} \quad (14)$$

These Debye lengths are those appropriate for the plasma at the material surface in steady state including the returning electrons. Since the local average electron energy divided by the number density increases with increasing distance from the surface, Equation 12 shows that the locally computed Debye lengths increase with distance from the surface.

These surface Debye lengths are shown in Figures 10a, b, and c.

For example, if a 10 keV blackbody is incident on silicon dioxide at  $0.8 \text{ cal/cm}^2/\text{ns}$ , Figure 10c shows  $\ell_D \approx 0.1 \text{ cm}$ . In this case the thickness of the boundary layer, as nearly as it can be defined, is at most a few millimeters. The number density and electric field profiles, shown in later sections, exhibit the actual structure of the layer.

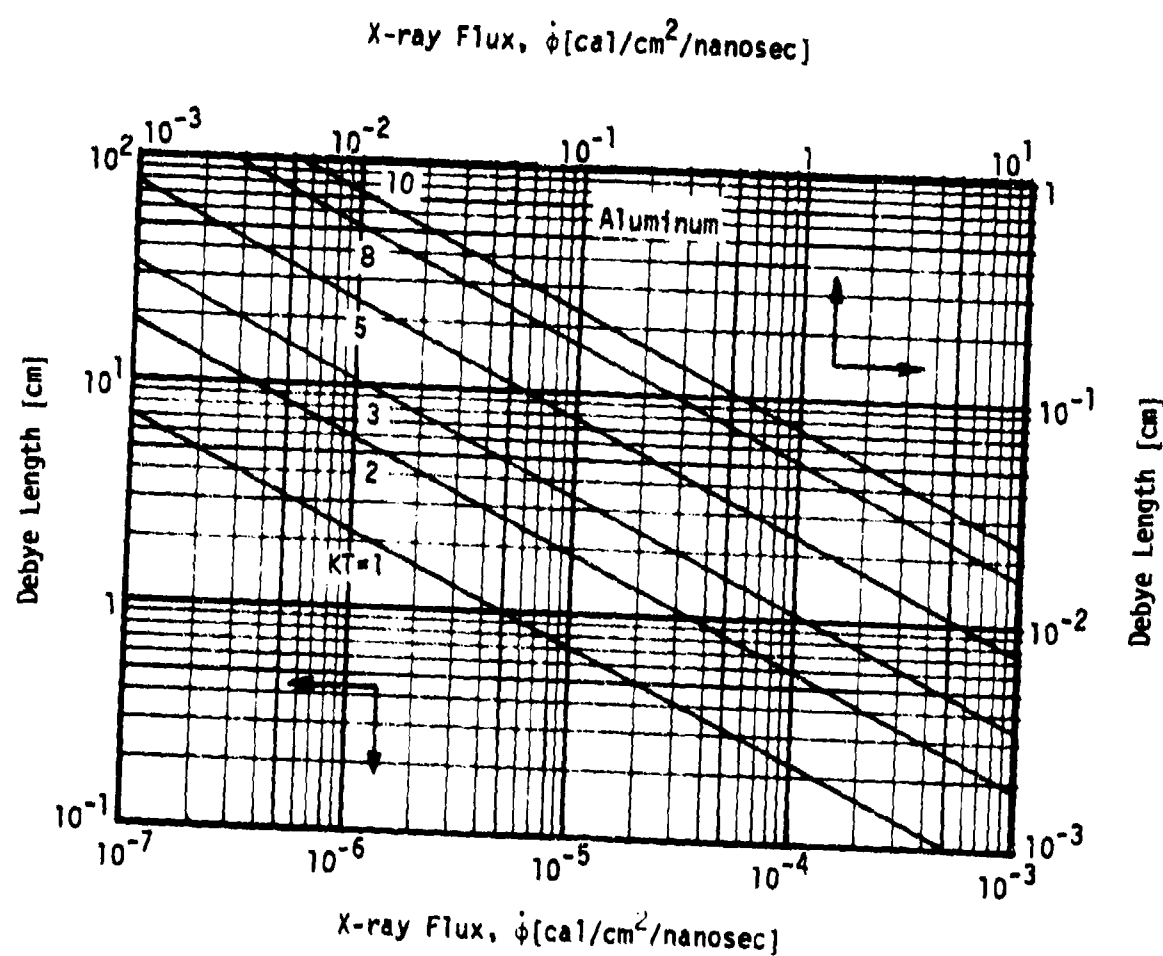


Figure 10a. Debye lengths for Aluminum.

Numbers on curves are blackbody temperatures in keV.

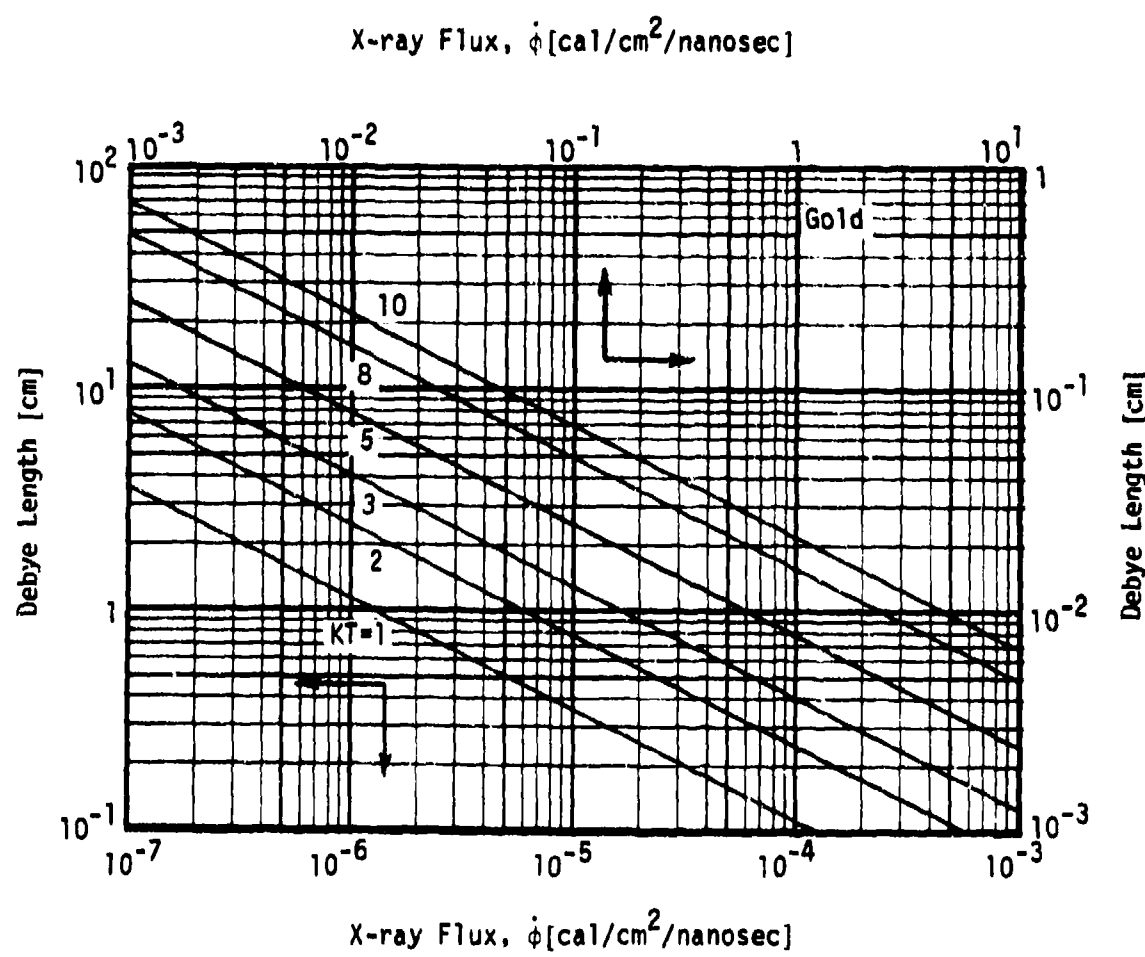


Figure 10b. Debye lengths for Gold.

Numbers on curves are blackbody temperatures in keV.

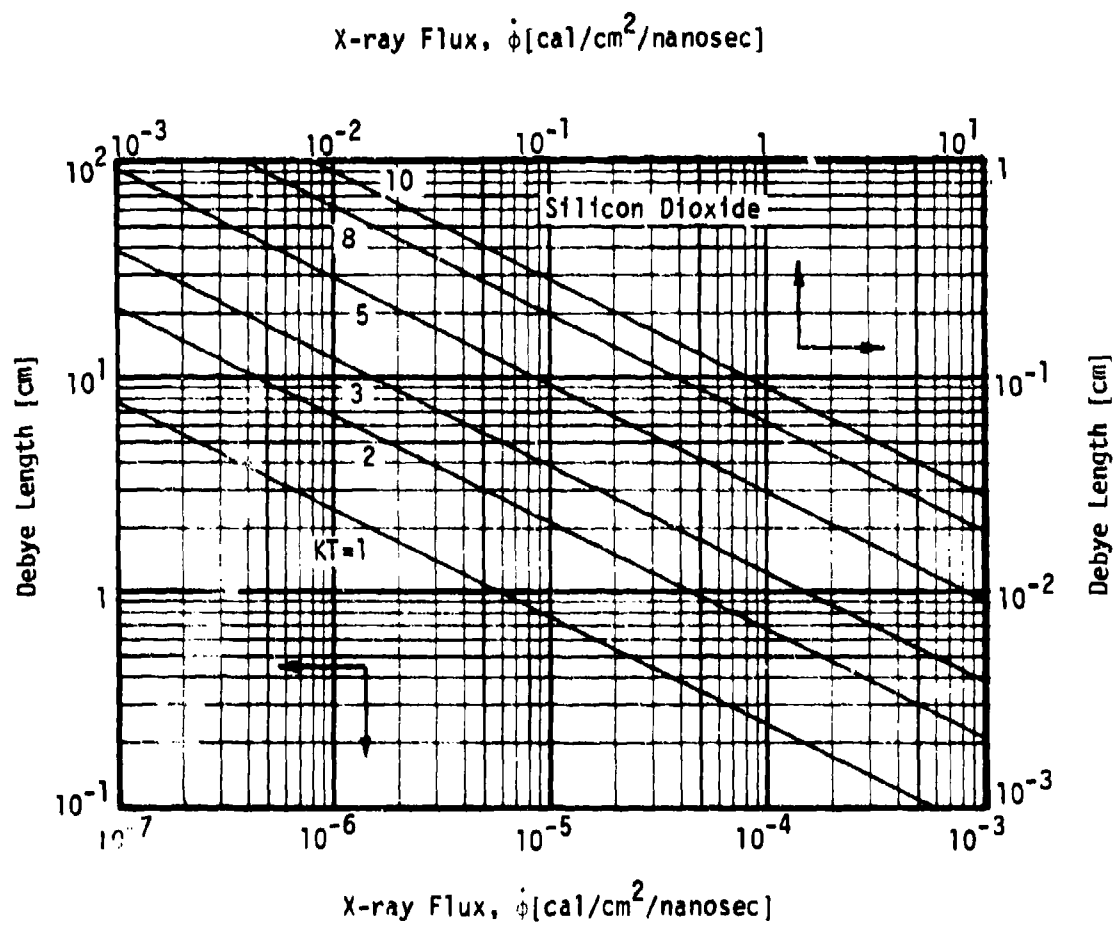


Figure 10c. Debye lengths for Silicon Dioxide.

Numbers on curves are blackbody temperatures in keV.

## SECTION 5

### ELECTRON NUMBER DENSITY AT SURFACE

We treat the electron number density  $N(x)$  as a function of distance  $x$  from the surface in two parts. We discuss first the density at the surface

$$N_{\text{surface}} \equiv N(x=0) \quad [\text{electrons/cm}^3], \quad (15)$$

and secondly the normalized profile  $N(x)/N(0)$ . This permits some simplification since the profile, when  $x$  is scaled to the Debye length, is a universal function. The profile is given in Section 6. The density at the surface is

$$\begin{aligned} N_{\text{surface}} &= 4\sqrt{\pi} \frac{r_0}{v_1} \\ &= 3.78 \frac{\gamma\left(\frac{\text{elec}}{\text{cal}}\right) \phi\left(\frac{\text{cal}}{\text{cm}^2 \text{ns}}\right)}{\sqrt{E_1(\text{keV})}} \quad [\text{cm}^{-3}], \end{aligned} \quad (16)$$

where  $v_1 = \sqrt{2E_1/m}$ . This is shown in Figures 11a, b, and c. It includes both the emitted and returning electrons.

For example if a 2 keV blackbody is incident on aluminum at a flux of  $3 \times 10^{-4} \text{ cal/cm}^2/\text{ns}$ , Figure 11a shows  $N_{\text{surface}} = 9.9 \times 10^9 \text{ electrons/cm}^3$ .

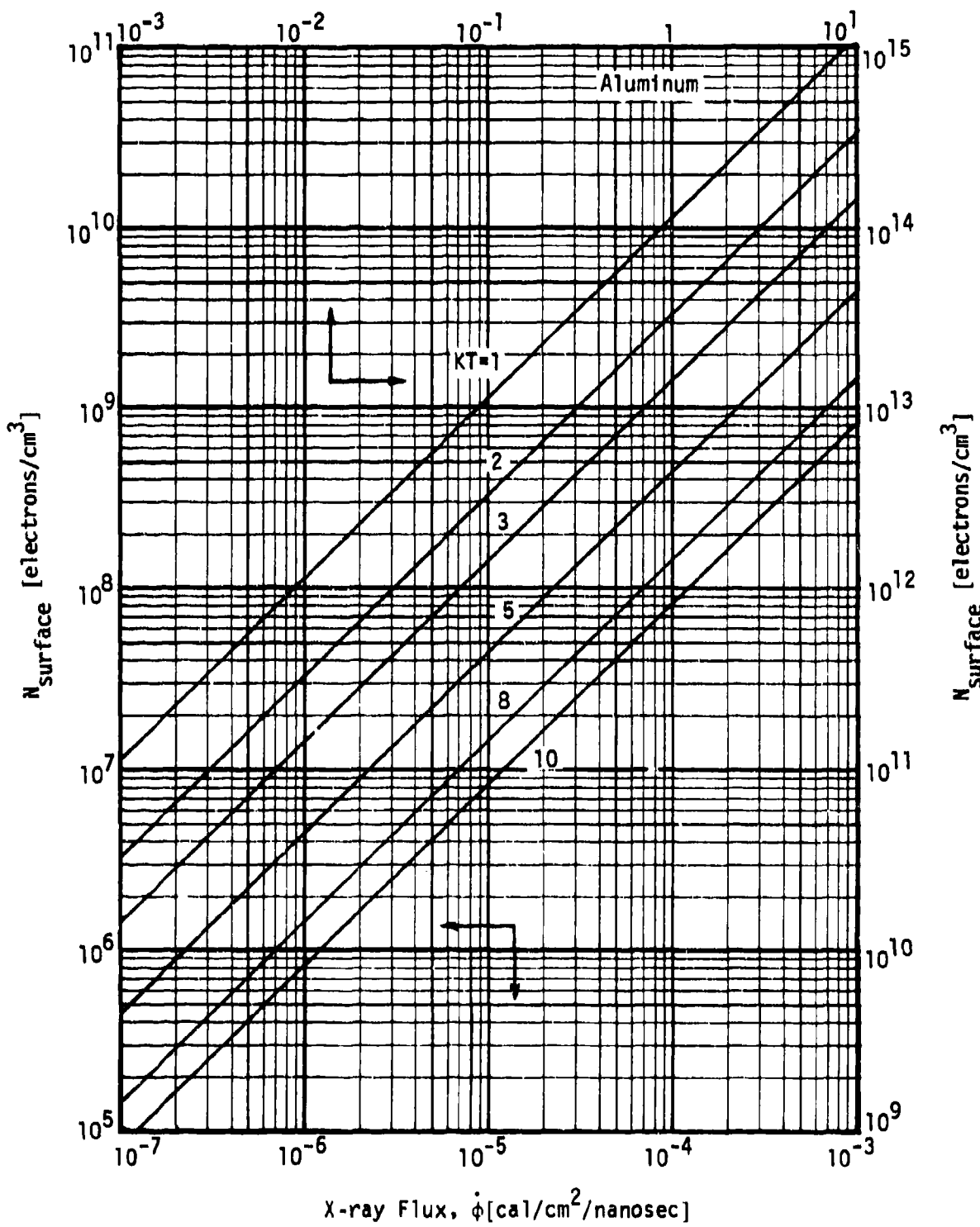


Figure 11a. Surface electron density for Aluminum.

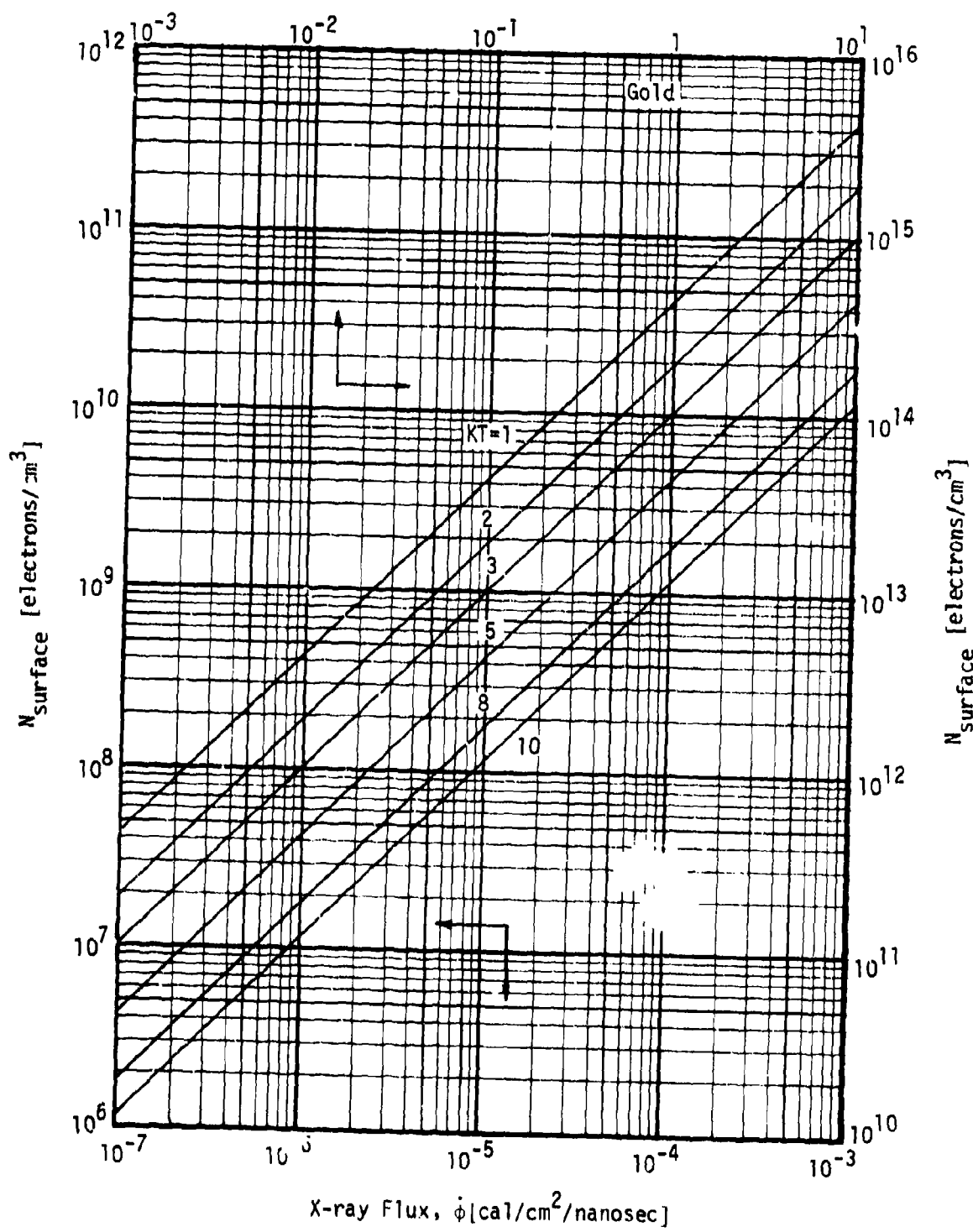


Figure 11b. Surface electron density for Gold.

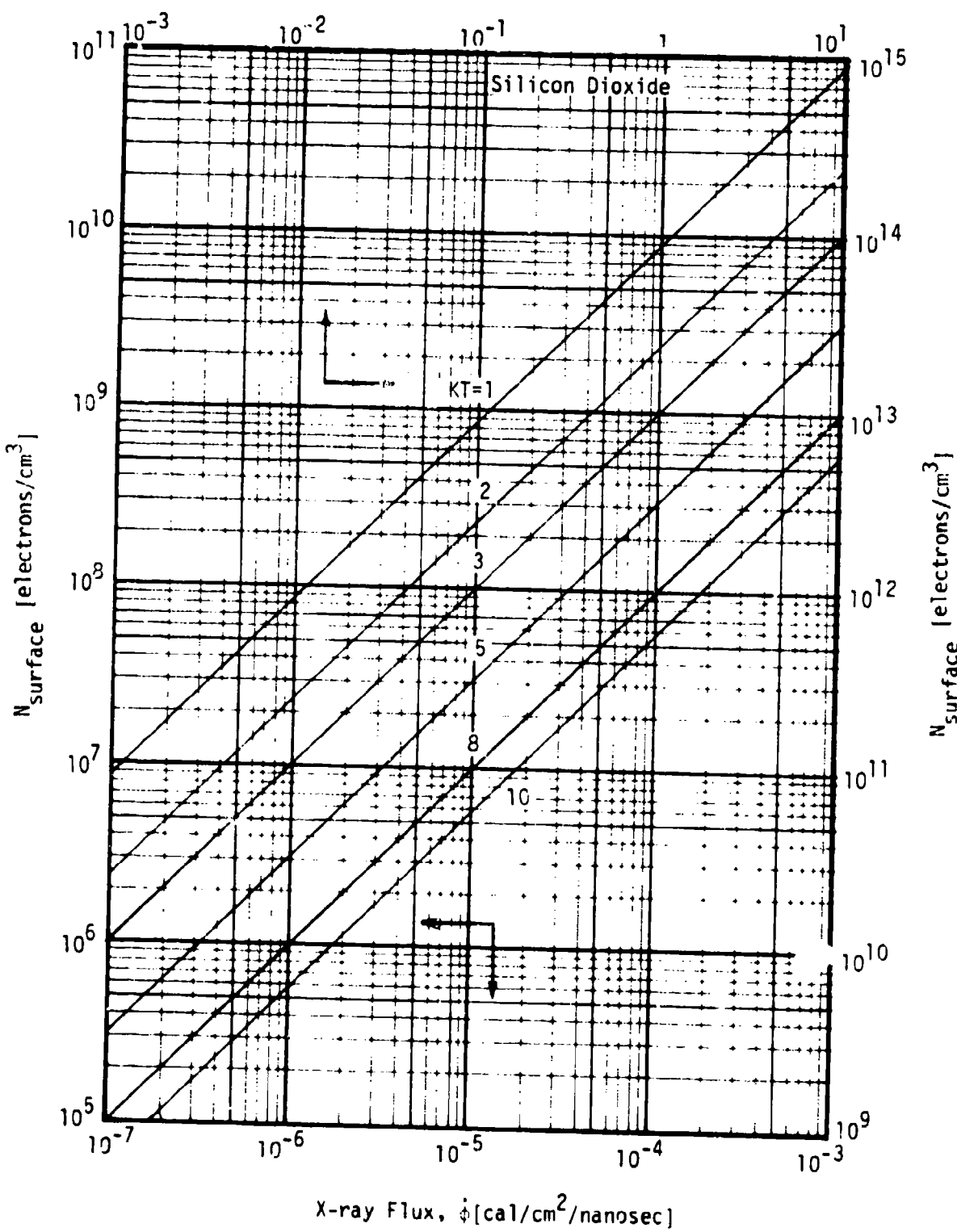


Figure 11c. Surface electron density for Silicon Dioxide.

## SECTION 6

### ELECTRON NUMBER DENSITY PROFILE

As mentioned in the last section we treat the electron number density  $N(x)$  as a function of distance  $x$  from the surface in two parts, its surface value, Equation 15, and its profile normalized to its surface value,  $N(x)/N(0)$ . If distance  $x$  is scaled to the Debye length, then  $N(x)/N(0)$  is a universal function of  $x/\ell_D$ .

The density profile is shown in Figure 12 on a linear scale out to 10 Debye lengths, by which point it is about 0.01 of its surface value, which is unity. This figure shows the true shape of the steady state number density for an exponential emission electron energy spectrum and  $\cos\theta$  angular distribution. It is taken from Reference 1. Its slope at the surface is divergent.

The number density drops to  $1/e$  of its surface value in about 0.54 Debye lengths. At two Debye lengths it is less than 0.1 of its surface value.

The profile is plotted again on a semi-log scale in Figure 13 out to 50 Debye lengths to show the larger distance behavior. As  $x \rightarrow \infty$ ,

$$\frac{N(x)}{N(0)} \xrightarrow{x \rightarrow \infty} \frac{2\ell_D^2}{x^2} . \quad (17)$$

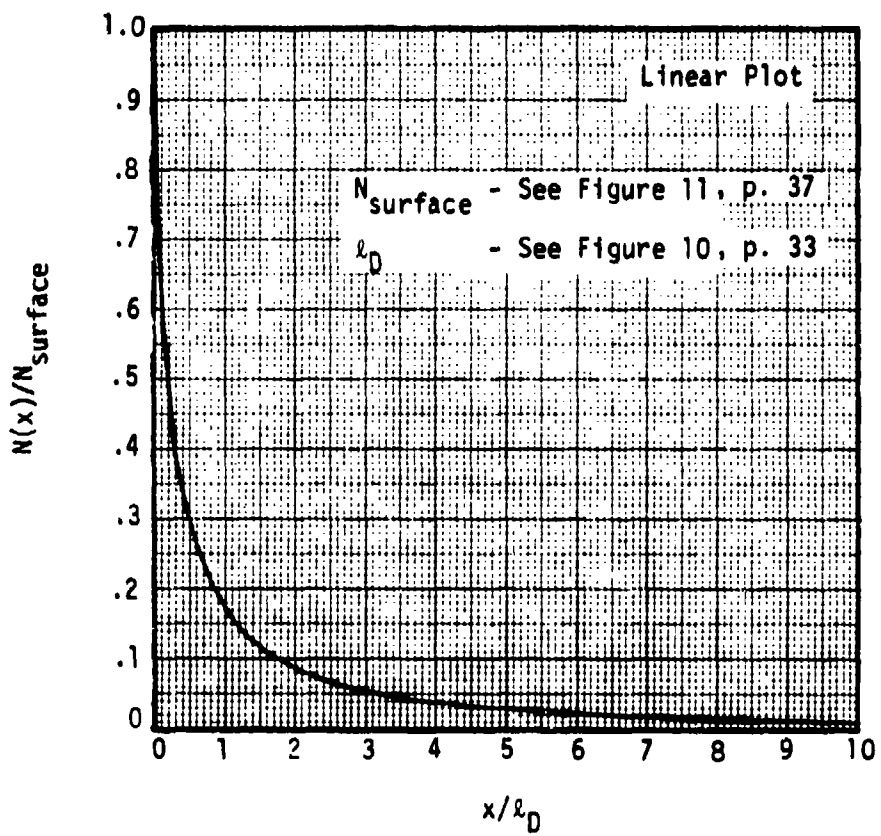


Figure 12. Normalized electron density profile.

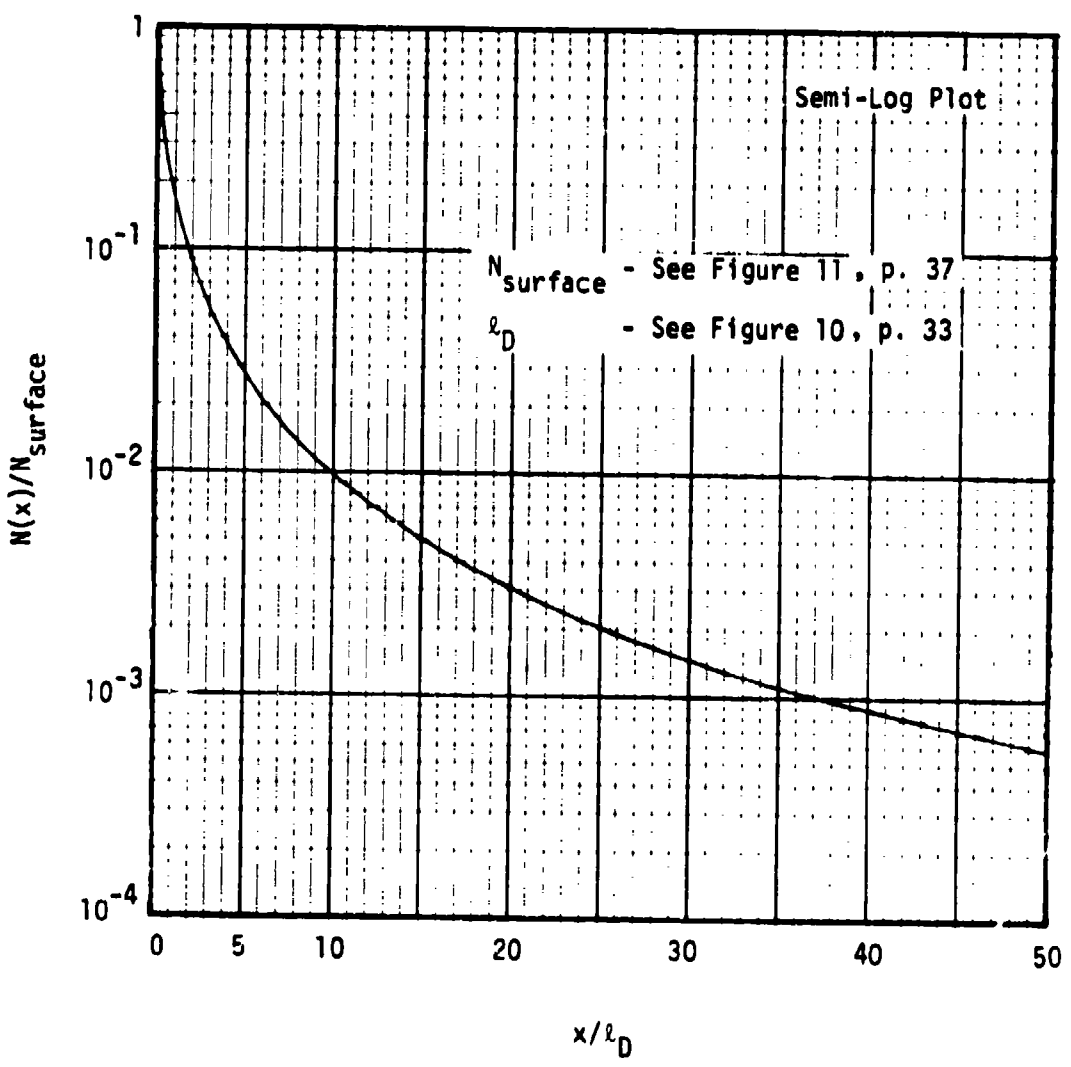


Figure 13. Normalized electron density profile.

## INTEGRATED NUMBER DENSITY

The integral of the number density out to  $x$ ,  $N_T(x)$ , gives the total number of electrons out to  $x$ ,

$$N_T(x) = \int_0^x N(x) dx \quad [\text{electrons/cm}^2] . \quad (18)$$

Gauss' law

$$\frac{\partial E}{\partial x} = 4\pi\rho = -4\pi eN(x) , \quad (19)$$

where  $e(>0)$  is the magnitude of the electron charge,  $E$  is the electric field, and  $\rho = eN$  is the charge density, can be used to express  $N_T(x)$  in terms of  $E(x)$ :

$$N_T(x) = \frac{E(0)}{4\pi e} \left(1 - \frac{E(x)}{E(0)}\right) . \quad (20)$$

Here,  $E(0)$  is the surface electric field, and  $E(0)/4\pi$  is the surface charge density.  $N_T(\infty) = E(0)/4\pi e$ . The fraction of electrons out to  $x$ ,  $N_T(x)/N_T(\infty)$ , is shown in Figure 14.

It shows, for example, that one half of the electrons are contained in the first 1.5 Debye lengths. The first Debye length contains about 41 percent of all the electrons. About 88 percent are contained in the first 14 Debye lengths.

The surface electric field itself,  $E(0) = E_{\text{surface}}$ , and the electric field profile  $E(x)/E(0)$  are shown in the next two sections.

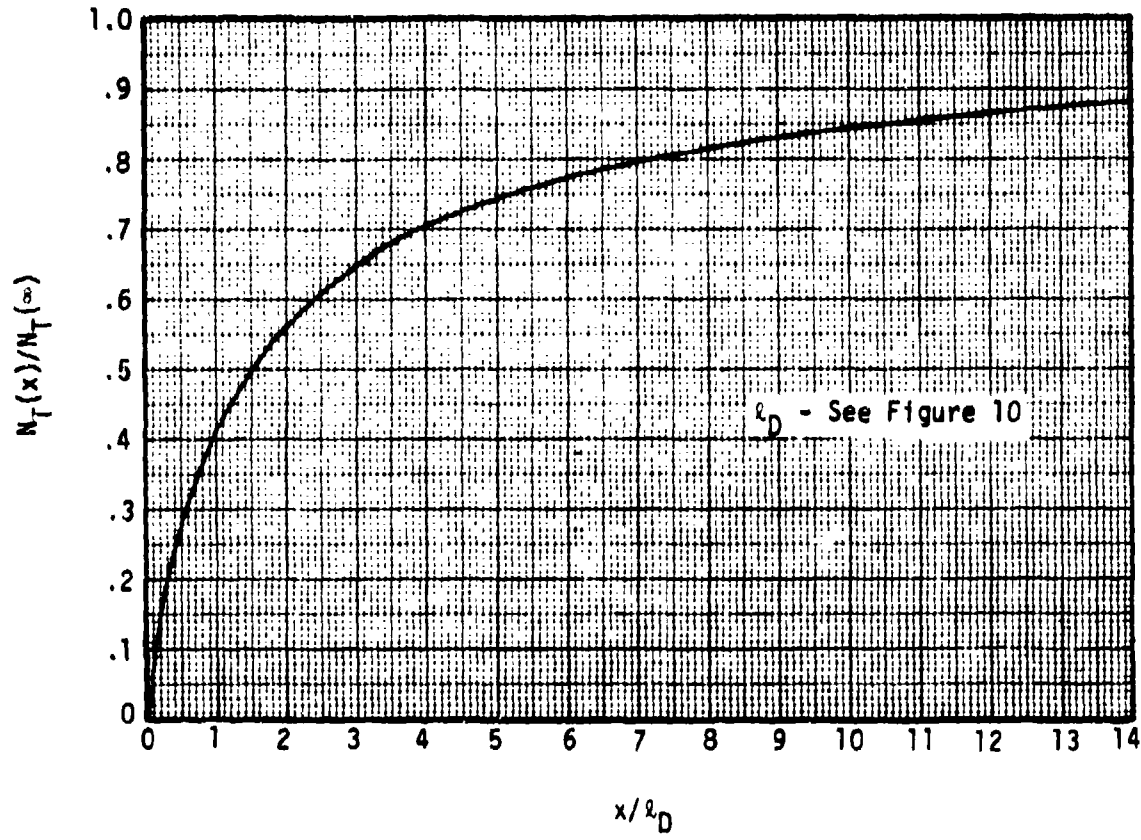


Figure 14. Fraction of electrons out to  $x$ .

## SECTION 7

### ELECTRIC FIELD AT SURFACE

We treat the electric field  $E(x)$  as a function of distance  $x$  from the surface also in two parts as we did the density. The surface electric field

$$E_{\text{surface}} = E(x=0) , \quad (21)$$

is given here. It also determines the surface charge density

$$\sigma = \frac{E_{\text{surface}}}{4\pi} , \quad (22)$$

and the total number of electrons

$$N_T = \frac{E_{\text{surface}}}{4\pi e} , \quad (23)$$

to which Figure 14 was normalized.

The surface electric field [volts/meter] is shown in Figures 15a, b, and c.

For example, a 1 keV blackbody incident on gold at 1 cal/cm<sup>2</sup>/nanosec produces a steady state field of about  $7.4 \times 10^7$  volts/meter (Figure 15b).

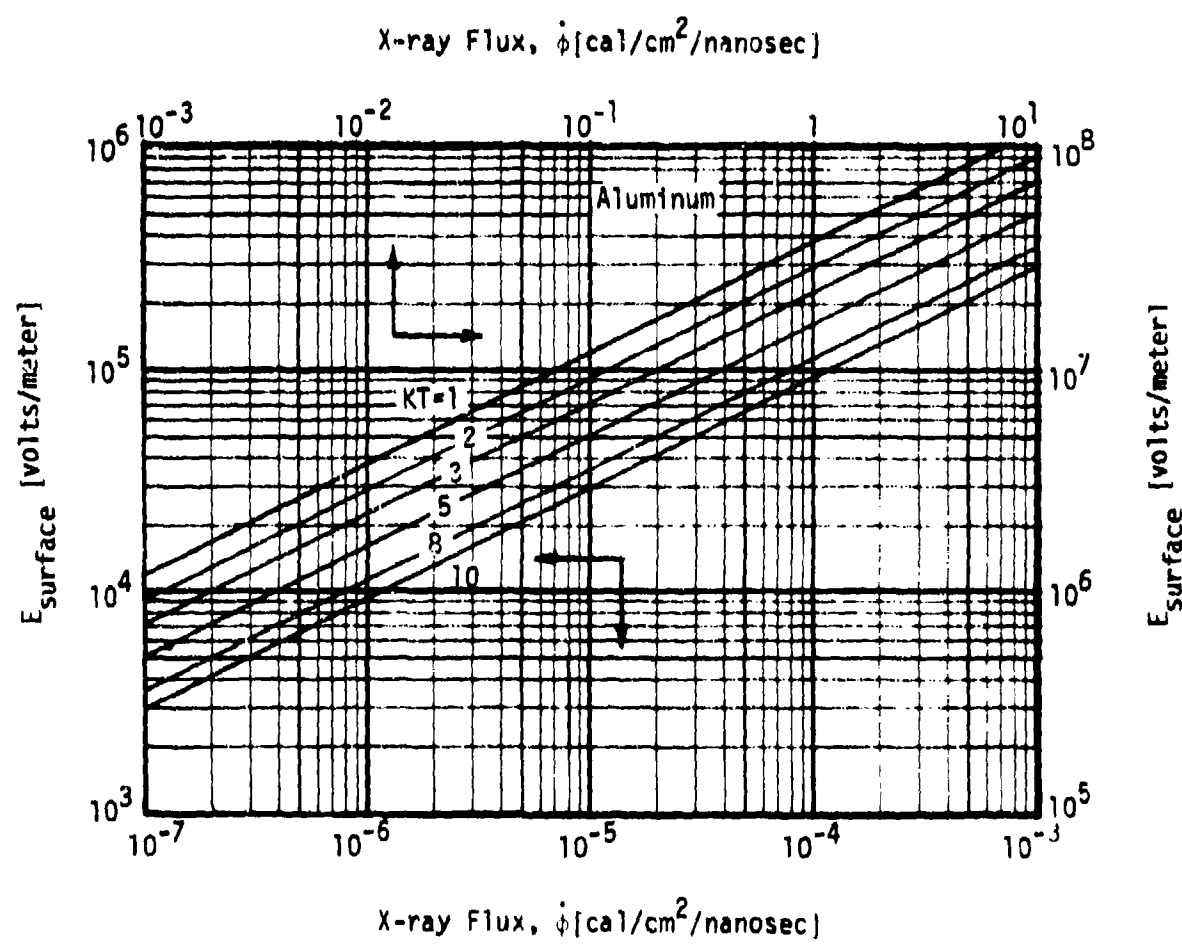


Figure 15a. Surface electric field for Aluminum.

Numbers on curves are blackbody temperatures in keV.

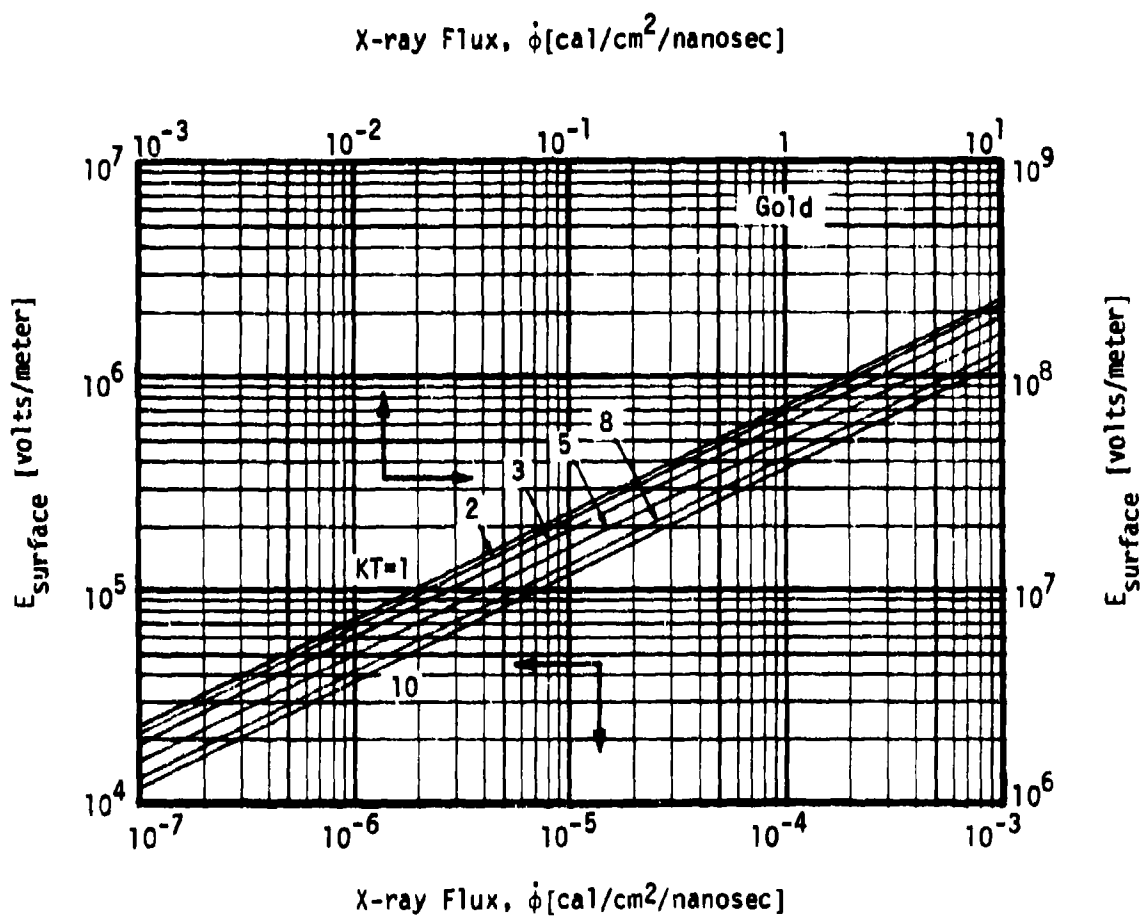


Figure 15b. Surface electric field for Gold.

Numbers on curves are blackbody temperatures in keV.

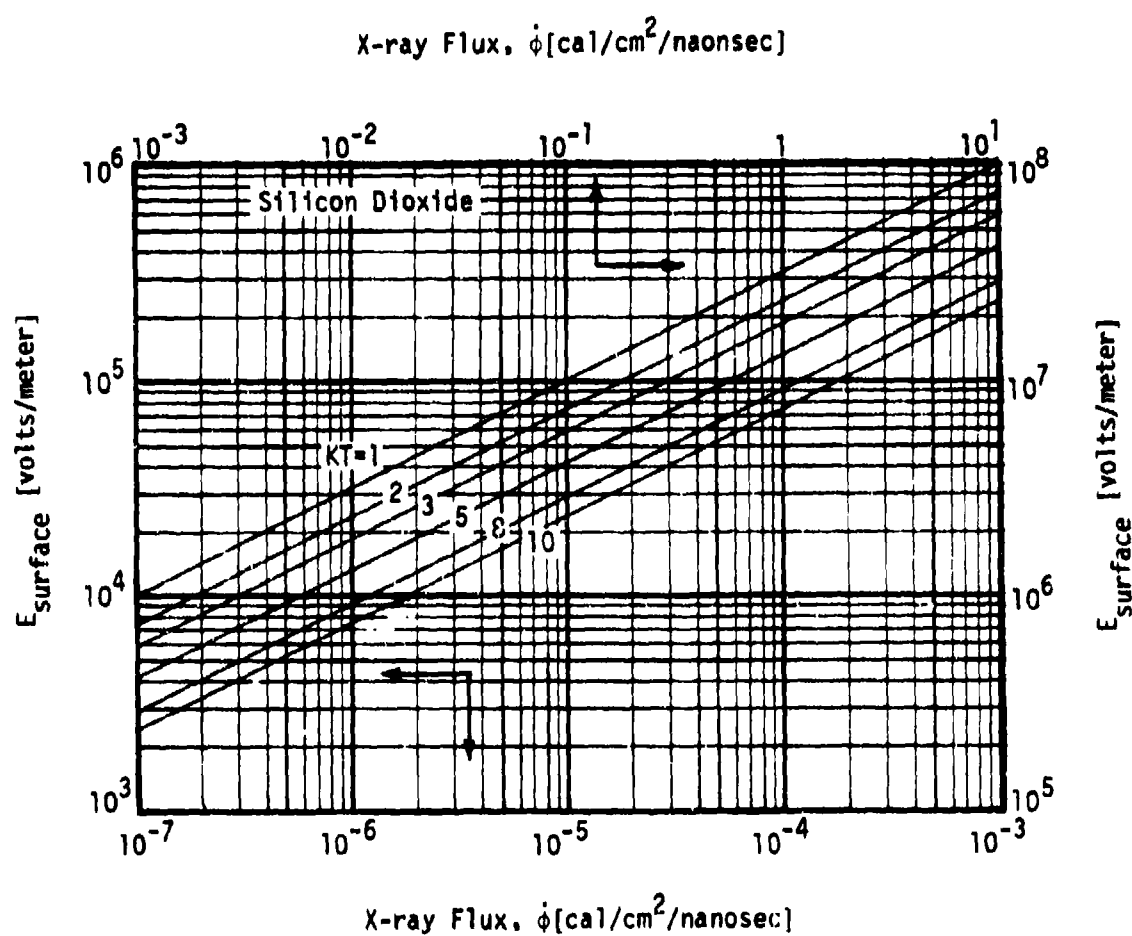


Figure 15c. Surface electric field for Silicon Dioxide.

Numbers on curves are blackbody temperatures in keV.

## SECTION 8

### ELECTRIC FIELD PROFILE

The electric field as a function of distance from the surface, normalized to its surface value,  $E(x)/E_{\text{surface}}$ , is shown in Figure 16.

As Equation 20 shows, this is one minus the total number of electrons. It drops to  $1/e$  of its surface value in about 2.8 Debye lengths.

Together with the surface field from Figures 15a, b, or c, and the Debye length from Figures 10a, b, or c, Figure 16 will give the electric field at any distance from the surface in steady state.

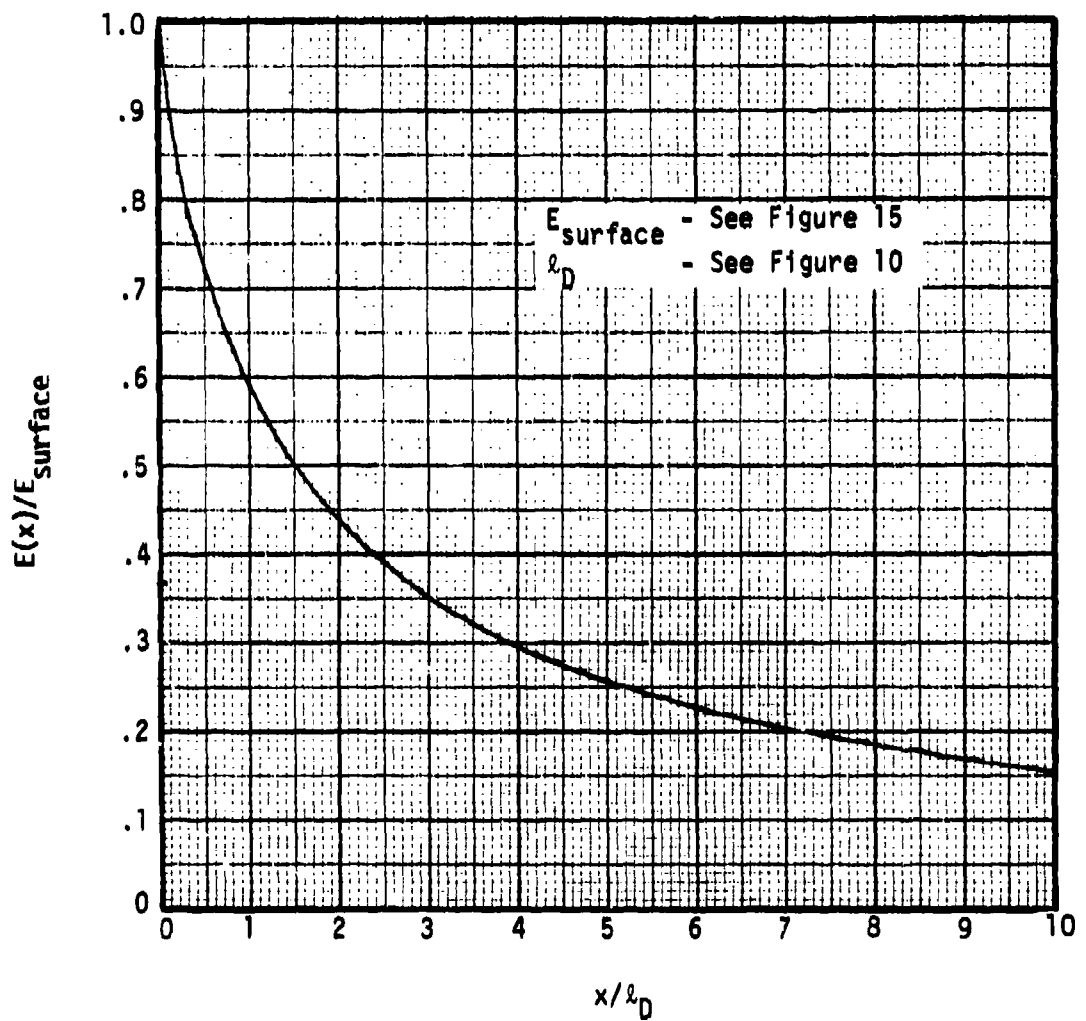


Figure 16. Normalized electric field profile.

## SECTION 9

### PLASMA FREQUENCY AT SURFACE

If  $N$  is the local electron number density ( $\text{cm}^{-3}$ ), the local plasma frequency is defined as

$$\omega_p = \sqrt{\frac{4\pi c^2}{m}} N \quad [\text{radians/sec}] . \quad (24)$$

We work instead with the frequency

$$f_p = \frac{\omega_p}{2\pi}$$
$$= \sqrt{\frac{e^2 N}{m}} \quad \text{Hz} . \quad (25)$$

We use the surface value of  $N$ , Equation 16, to obtain the surface plasma frequency

$$f_p = 1.746 \times 10^4 \left( \frac{Y(\text{elec}) \phi \left( \frac{\text{cal}}{\text{cm}^2 \text{ns}} \right)}{\sqrt{E_1(\text{keV})}} \right)^{1/2} \quad \text{Hz} . \quad (26)$$

This is shown in Figures 17a, b, and c.

For example an 8 keV blackbody on silicon dioxide at  $10^{-4} \text{ cal/cm}^2/\text{ns}$  produces a surface plasma frequency of  $9 \times 10^7 \text{ Hz}$ .

The local plasma frequency at a distance from the surface drops off as the square root of the number density, that is, as the square root of the ordinate in Figures 12 or 13.

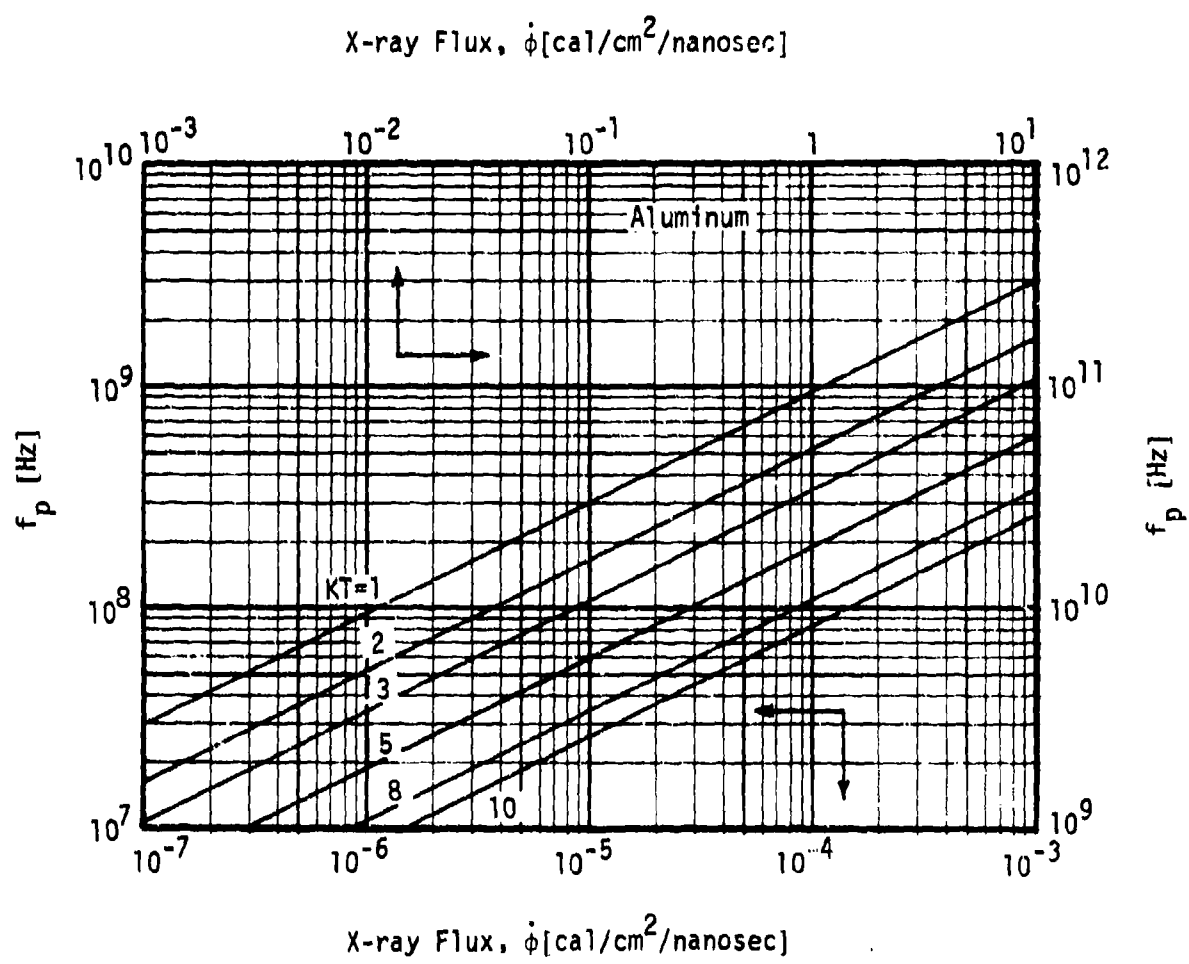


Figure 17a. Surface plasma frequency for Aluminum.

Numbers on curves are blackbody temperatures in keV.

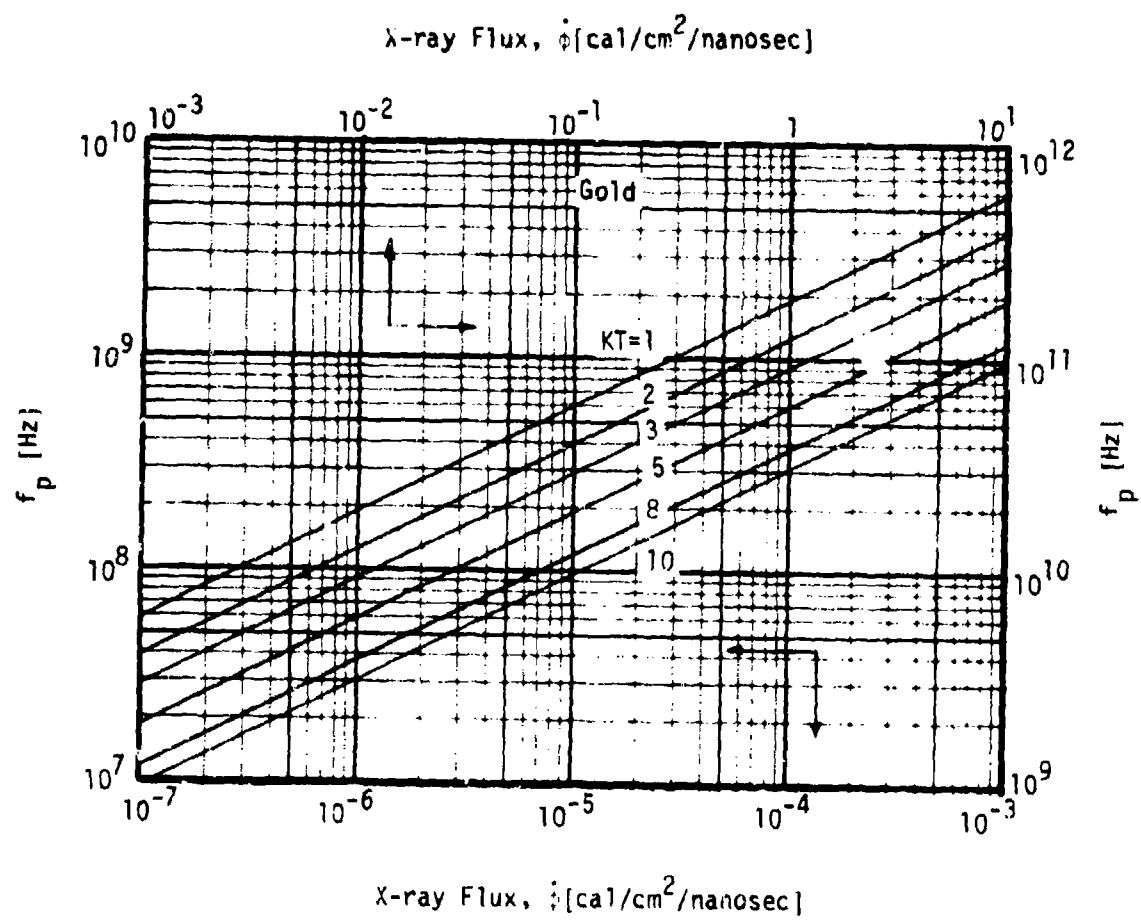


Figure 17b. Surface plasma frequency for Gold.

Numbers on curves are blackbody temperatures in keV.

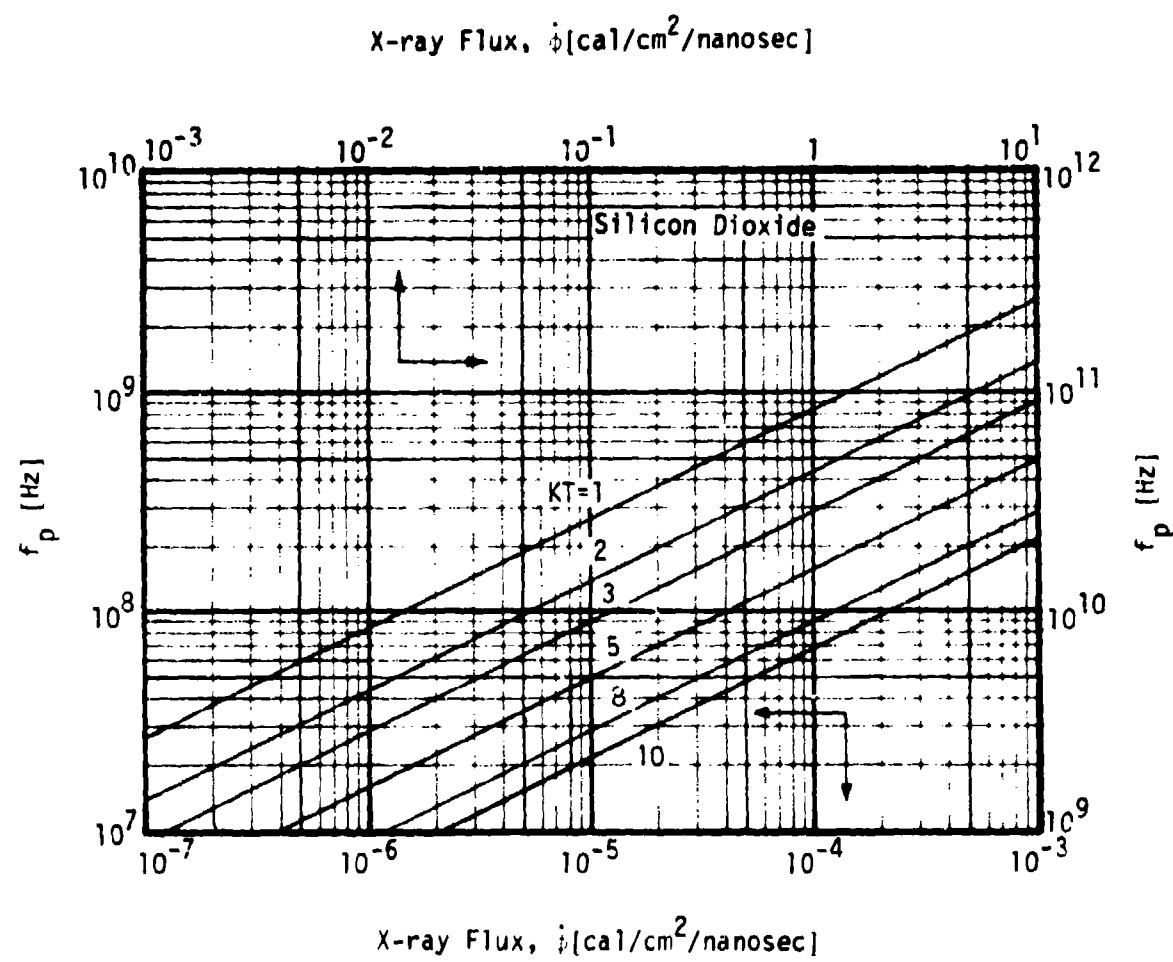


Figure 17c. Surface plasma frequency for Silicon Dioxide.

Numbers on curves are blackbody temperatures in keV.

## SECTION 10

### DIPOLE MOMENT PER UNIT AREA

In Gaussian cgs units, the electric dipole moment of the layer contributed by all electrons out to  $x$  is

$$P(x) = \int_0^x x\rho(x) dx \text{ esu-cm/cm}^2 . \quad (27)$$

Reference 1 shows this to be proportional to a universal dimensionless function,  $\Phi(x/\ell_D)$ , of  $x/\ell_D$ :

$$P(x) = \frac{E_1}{4\pi c} \Phi(x/\ell_D) \text{ esu/cm} , \quad (28)$$

where  $E_1$  (ergs) is the electron exponentiation energy which was given in keV in Table 2. If  $E_1$  is written in keV, and  $P(x)$  in MKS units, Equation 28 becomes

$$P(x) = 8.854 \times 10^{-9} E_1 (\text{keV}) \Phi(x/\ell_D) \frac{\text{Coulombs}}{\text{meter}} . \quad (29)$$

Hence the quantity

$$\frac{P(x)}{E_1 (\text{keV})} \left[ \frac{\text{Coulombs}}{\text{meter-keV}} \right] \quad (30)$$

is a universal function of  $x/\ell_D$ . It is shown plotted in Figure 18.

To use Figure 18 for a certain blackbody spectrum on a particular material, first obtain  $E_1$  from Table 2, and the Debye length from Figure 10a, b, or c. Then to obtain the dipole moment out to  $x$ , multiply  $E_1$  (keV) by the ordinate in Figure 18 at the correct value of  $x/\ell_D$ .

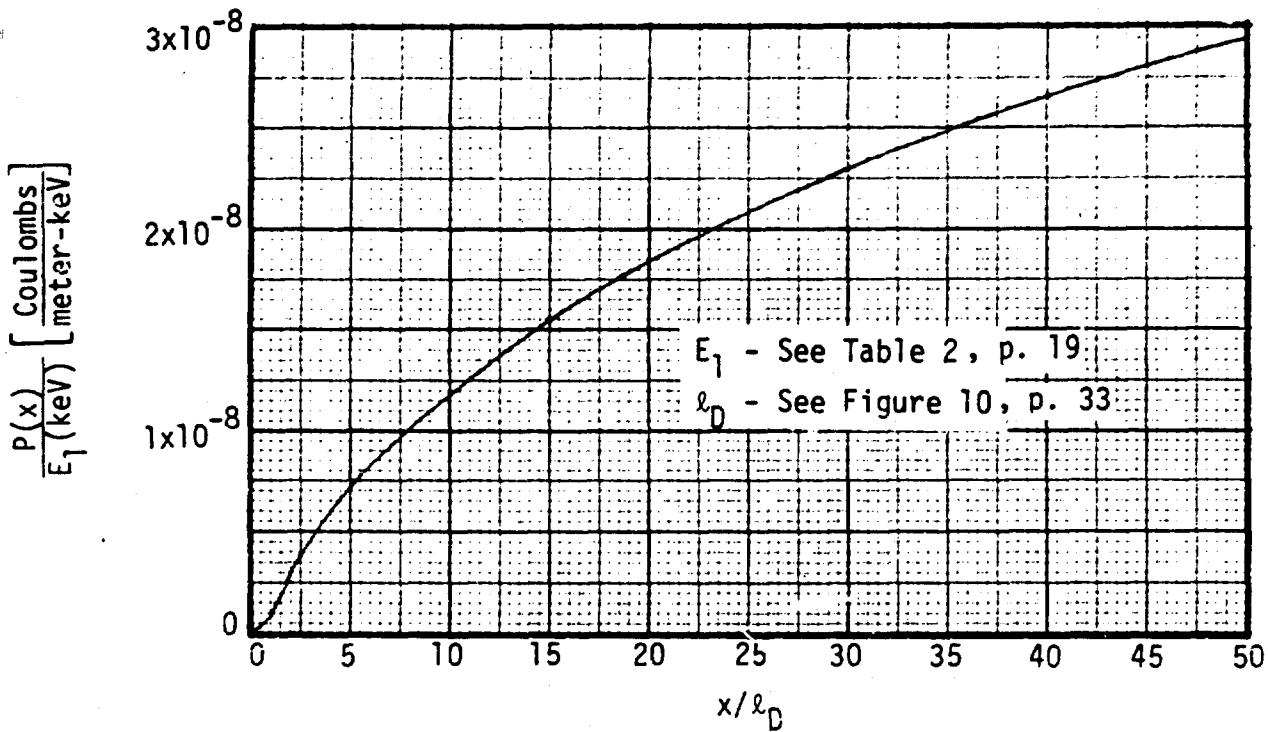


Figure 18. Normalized dipole moment per unit area.

For example for a 10 keV blackbody incident on gold at  $10^{-1}$  cal/ $\text{cm}^2/\text{nanosec}$ , Table 2 shows  $E_1 = 10.07 \text{ keV}$ , and Figure 10b shows  $l_D = 0.07 \text{ cm}$ . Then Figure 18 shows that electrons out to, say,  $x = 1 \text{ cm}$  ( $x/l_D = 14.3$ ), where the ordinate is  $1.5 \times 10^{-8}$ , contribute a dipole moment of

$$\begin{aligned}
 P(x=1 \text{ cm}) &= 10.07 \times 1.5 \times 10^{-8} \\
 &= 1.51 \times 10^{-7} \text{ Coul/meter}. \quad (31)
 \end{aligned}$$

Estimates such as this for the dipole moment are useful for determining distant electric dipole fields produced by the layer.

The dipole moment diverges for large  $x$ . This is because the charge density  $\rho$  in Equation 27 drops off as  $x^{-2}$  so the integral diverges logarithmically. The electrostatic potential also diverges. The divergence is due to the exponential spectrum which contains electrons of arbitrarily high velocity, and is a theoretical artifact.

To obtain a meaningful estimate for a real situation the following procedure is suggested. At the time  $P(x)$  is desired, estimate the maximum distance the most energetic electron traveling at less than the speed of light could have gone. Determine  $P$  at this distance from Figure 18. Since  $P$  increases slowly with distance, remaining of order a few times  $10^{-8}$  Coulombs/meter for many Debye lengths, the exact distance  $x$  is not too critical for rough estimates.

To convert  $P(x)$  to esu, use

$$1 \frac{\text{Coulomb}}{\text{meter}} = 3 \times 10^7 \frac{\text{esu}}{\text{cm}}$$

BEST AVAILABLE COPY

## SECTION 11 EXAMPLE

We discuss an example here to illustrate the use of all graphs.

We consider as an example a 5 keV blackbody spectrum incident on aluminum with a time history as shown in Figure 19, and a fluence of 1 cal/cm<sup>2</sup>. This information, the incident spectrum, the target material, the time history, and the fluence, we assume given.

Irrespective of the time history and fluence, Table 1 (or Figure 1) shows the backscattered electron yield to be

$$Y = 2.57 \cdot 10^{12} \frac{\text{electrons}}{\text{calorie}} . \quad (32)$$

Figure 5 shows the approximate electron energy spectrum (for electrons of energy greater than 1 keV) and Table 2 shows that the spectrum is nearly exponential with exponentiation energy.

$$E_1 = 4.77 \text{ keV} . \quad (33)$$

The emission angular spectrum (per steradian) is approximately proportional to  $\cos^2\theta$ , where  $\theta$  is the emission angle measured from the normal.

To estimate the time  $t_s$  after which we may use steady state theory (and therefore all the graphs in this report), we need  $\dot{I}$  at early times. This is obtained from Figure 19.

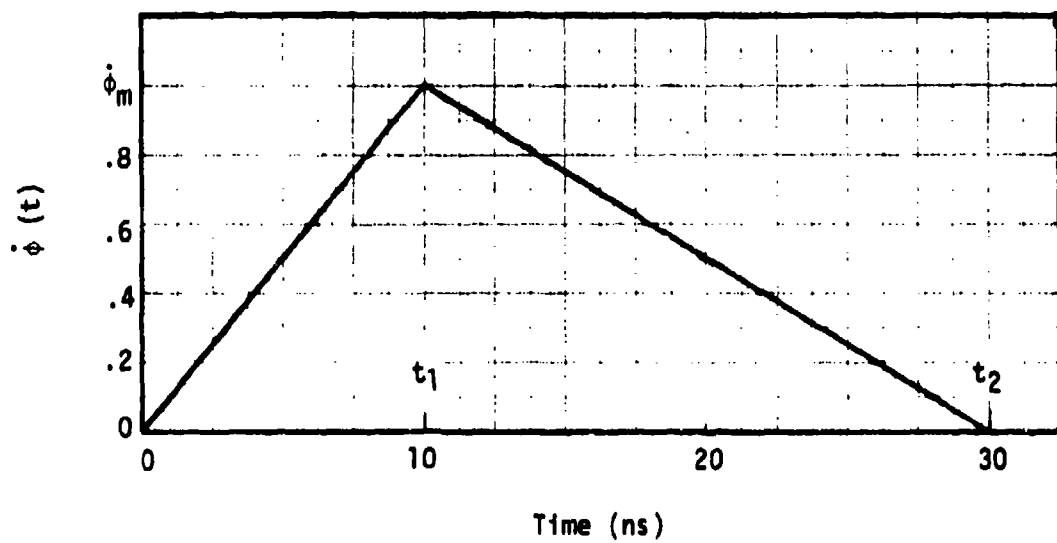


Figure 19. X-ray time history for illustrative example.

The maximum flux,  $\dot{\phi}_m$ , is determined from the fluence  $\phi$  by

$$\begin{aligned}\phi &= \int_0^\infty \dot{\phi} dt \\ &= \frac{1}{2} \dot{\phi}_m t_2\end{aligned}$$

so that

$$\dot{\phi}_m = \frac{2\phi}{t_2} = 6.67 \times 10^{-2} \text{ cal/cm}^2/\text{ns}. \quad (34)$$

Then

$$\dot{\phi} = \frac{\dot{\phi}_m}{t_1} = 6.67 \times 10^{-3} \text{ cal/cm}^2/\text{ns}^2. \quad (35)$$

From Figure 8a we determine

$$t_s \approx 0.9 \text{ ns}. \quad (36)$$

Thus after about one nanosec we can expect to be in quasi-steady state.

To see if we sensibly remain in instantaneous steady state, we must have the flux change only slightly in the time  $t_{ret}$ , determined from Figure 9a and an average  $\dot{\phi}$  of, say,  $\dot{\phi}_m/2 \approx 3 \times 10^{-2} \text{ cal/cm}^2/\text{ns}$ . Figure 9a shows

$$t_{ret} = 0.28 \text{ ns}. \quad (37)$$

During these times, Figure 19 shows the flux does change only slightly, so we may expect sensible estimates from all remaining graphs.

The Debye length, Figure 10a, shortens in time as  $\dot{\phi}$  increases, and then lengthens again as  $\dot{\phi}$  decreases after its peak. Its smallest value is when  $\dot{\phi} = \dot{\phi}_m$ , Equation 34, for which Figure 10a shows

$$l_{D,\text{minimum}} = 9.5 \times 10^{-2} \text{ cm} . \quad (38)$$

The surface number density increases with  $\dot{\phi}$  to a maximum of

$$N_{\text{surface,max}} = 3 \times 10^{11} \text{ elec/cm}^3 , \quad (39)$$

when  $\dot{\phi} = \dot{\phi}_m$ , as shown by Figure 11a.

The number density profile is shown in Figure 12 or 13, and the fractional integrated number in Figure 14. Figure 14 shows 75 percent of the electrons inside 5.2 Debye lengths, or within about 0.5 cm at time  $t = 10$  ns.

The surface field increases as the square root of  $\dot{\phi}$  to a maximum of

$$E_{\text{max}} = 4 \times 10^6 \text{ v/m} , \quad (40)$$

at 10 ns, as read from Figure 15a.

The electric field profile is shown in Figure 16.

The surface plasma frequency increases as the square root of the flux reaching a maximum at 10 ns of

$$f_{\nu,\text{max}} = 5 \times 10^9 \text{ Hz} , \quad (41)$$

as determined from Figure 17a.

The dipole moment out to 50 Debye lengths ( $\approx 4.8$  cm using the minimum  $l_D$ , Equation 38) is shown in Figure 18 to be about

$$\begin{aligned} P &\approx E_1 (\text{keV}) \times 3 \times 10^{-8} \\ &= 1.4 \times 10^{-7} \text{ Coulombs/meter} , \end{aligned} \quad (42)$$

which is about 4.3 esu/cm.

BEST AVAILABLE COPY

REFERENCES

1. Carron, Neal J., and C. L. Longmire, On the Structure of the Steady-State, Space-Charge-Limited Boundary Layer in One Dimension, Mission Research Corporation, MRC-R-240, November 1975.
2. Dellin, T. A., and C. J. MacCallum, QUICKE2: A One-Dimensional Code for Calculating Bulk and Vacuum Emitted Photo-Compton Currents, Sandia Laboratories, SLL-74-0218, April 1974.
3. Higgins, D. F., X-ray Induced Photoelectric Currents, Mission Research Corporation, MRC-R-81, June 1973.